Theoretical methods for the relativistic atomic many-body problem

J. Sapirstein

Department of Physics, University of Notre Dame, Notre Dame, Indiana 46556

Because of the well-understood nature of the electromagnetic interaction, the presence of a well-defined center of force, and the relative unimportance of nonperturbative effects, the atomic many-body problem is argued to be an ideal laboratory for the study of high-accuracy theoretical many-body techniques. In particular, the convergence of many-body perturbation theory (MBPT) for highly charged ions is so rapid that the relativistic generalization of the Schrödinger equation can be accurately solved with MBPT through second order. Relatively large radiative corrections in these ions require the integration of QED and MBPT, which can be accomplished by using S-matrix theory. However, to reach high accuracy for neutral atoms, methods based on summation of infinite classes of MBPT diagrams are required. Both RPA and Brueckner-orbital-type summations are needed to reach the one-percent level for heavy atoms, and to proceed further the need for the evaluation of new classes of diagrams involving triple excitations will be described. [S0034-6861(98)00801-0]

CONTENTS

I. INTRODUCTION

The basic atomic many-body problem is that of the solution of $H\psi = E\psi$, where $H = H_0 + V$, with

$$H_0 = \sum_{i=1}^{N} \frac{\vec{p}_i^{\,2}}{2m} - \sum_{i=1}^{N} \frac{Z\alpha}{r_i} \tag{1}$$

and

$$V = \frac{\alpha}{2} \sum_{i \neq j} \frac{1}{|\vec{r}_i - \vec{r}_j|} \, . \tag{2}$$

Equations of this form are used as the starting point for a wide range of physical problems: a great deal of chemistry, atomic physics, nuclear physics, equilibrium statistical mechanics, and condensed-matter physics all stems from variants of this equation. A common diagrammatic language is used to describe the associated perturbation theory and, in principle, provides a unified approach to these fields. In practice, however, the individual characteristics of the physics of the different fields tends to make for a marked nonuniformity in approach. In nuclear physics, for example, a reformulation of the perturbation expansion forced by large short-range forces is carried out early on, and in condensed-matter physics one is often interested in ground states that cannot be reached at all from perturbation theory. It is the purpose of this review to show how the many-body problem works in atomic physics, which is the field of physics in which it should be expected to be tested with the highest precision.

Briefly, the main characteristic of the atomic many-body problem is that ordinary many-body perturbation theory (MBPT) that starts from a Hartree-Fock potential works rather well for "simple" atoms and ions. By simple we mean either closed-shell systems or systems with one electron outside a closed shell. We shall discuss more complicated atoms in the next section. In the particularly interesting case of highly charged ions, working through second-order MBPT gives solutions so accurate that quantum electrodynamic (QED) corrections are clearly seen in the difference between MBPT and experiment. Even in neutral atoms MBPT through second order can give results accurate at the percent level. However, to reach further accuracy, the same infinite subsets of MBPT diagrams that play such important roles in nuclear and condensed-matter physics must be considered.

The atomic many-body problem is unique as a system in which to test many-body methods. It is most similar to quantum chemistry and can be thought of as a branch of that field. However, because the atomic problem has a single center of force, spherical symmetry can be used to reduce greatly the number of wave functions that have to be considered. For example, although cesium has 55 electrons, only 12 radial functions are needed to describe the atom nonrelativistically. The practical effect of this is that the basis sets, whose use in carrying out atomic calculations will be described in Sec. III C, can be chosen to be large enough so that the associated basis-set truncation error is negligible.

Turning to a comparison with nuclear physics, we note the advantage of there being no uncertainty whatsoever

about the nature of the interaction, as the underlying theory of atomic and molecular structure is QED. Regardless of the completeness with which the Schrödinger equation is solved in the nuclear problem, there will be uncertainties associated with the exact form of the nucleon-nucleon interaction and the role of three-body forces, at least until quantum chromodynamics becomes a practical calculational tool. [Three-body forces exist in atomic physics, but as small and calculable QED effects (Zygelman, 1989; see also Mittelman, 1971, 1989).] We have already mentioned the fact that strong short-range forces require a rearrangement of perturbation theory for nuclear physics. In atomic physics no such rearrangement is necessary, although Brueckner-orbital-type corrections will be shown to play an important role when treated perturbatively. The tensor interactions present in the nuclear problem are also present in atomic physics, but they are well understood in the framework of QED, corresponding to the exchange of a transverse photon in Coulomb gauge, and are relatively small. A final simplification is the absence of pairing forces.

The atomic many-body problem is also free of the nonperturbative physics that affects many of the most interesting condensed-matter problems such as superconductivity, many magnetism problems, and certain transport problems like the Kondo effect, localization, and the quantum Hall effect. In these cases one cannot adiabatically continue from a picture of noninteracting particles to the relevant regime. Even in the cases where ordinary perturbation theory suffices to describe the physics of the solid state, there are uncertainties in the position of bands, effective electron masses, and lifetimes. Of course, the atomic many-body problem does not have the simplicity of Bloch waves for the Hartree-Fock solutions, but atomic Hartree-Fock wave functions and their related finite basis sets can be formed very quickly on modern computers, so this is not a practical problem.

While the dominant electromagnetic force in atoms is completely understood, there are uncertainties stemming from nuclear effects, though they are quite small. The finite size of the nucleus alters energy levels of penetrating states, and so, to the extent nuclear sizes are unknown, energy levels are uncertain. The finite mass of the nucleus can be accounted for by using the reduced mass, but higher-order recoil effects, as well as QED effects in general, have not been studied in the many-electron case to the same extent as in hydrogenic systems. In fact, these latter effects are from the point of view of quantum field theory perhaps the most interesting feature of atomic physics, and in a sense the atomic many-body problem is a background effect that needs to be eliminated so that the behavior of QED in many-electron systems can be studied.

Over the years a large arsenal of theoretical techniques has been developed to deal with the many-body problem. A very readable overview is given by Bishop and Kummel (1987). The technique described in this review is that of MBPT and extensions of it that sum infinite classes of diagrams. There exists a particular atomic physics problem that has determined this choice, which requires calculations of energy levels and matrix elements of heavy atoms accurate at the one-part-per-thousand level. This problem is the theoretical prediction of parity-nonconserving processes in cesium, lead, thallium, and bismuth. Recent reviews of this subject have been given by Sapirstein (1996) and Martensson-Pendrill (1992). To interpret the experimental results, which have recently reached the level of a few tenths of a percent in cesium (Wood *et al.*, 1997), one must understand the wave function beneath this level. The reason for the importance of this problem is that electroweak radiative corrections, which are sensitive to physics at the TeV level, enter at the percent level. Any deviations between theory and experiment can shed light on the question of possible new physics at this level, a central interest of modern particle physics. Because this process involves very small distances (the parity nonconservation arises from exchange of a Z between the nucleus and the electrons), this particular problem must be treated relativistically, so we shall always incorporate relativity from the start. This is easily done in MBPT; it should be noted, however, that most of the many-body issues we shall be concerned with are equally applicable to the nonrelativistic case. Secondly, the experiments involve excited states of open-shell atoms, with the experiments in cesium, for example, involving a transition between the $6s$ and $7s$ states. A large portion of the many-body literature is limited to calculations of the closed-shell case, and only the smaller portion on open-shell methods is applicable to this problem. Finally, because the issue of accuracy is so central, we require a method that can be systematically improved. We shall see that, while MBPT is such a method, with more and more physics included with each successive order of perturbation theory, the systematic improvement needed comes from reordering perturbation theory in terms of how many electrons are excited from the valence and core. This reordering involves the summation of infinite classes of MBPT diagrams, and we refer to any method that sums such classes as an *all-orders method*. The method we describe below is closely related to the *coupled-cluster methods* described by Bishop and Kummel (1987) and Bartlett (1991).[1]

The organization of this review is as follows. Because the main emphasis will be on relativistic MBPT and QED issues, the next section presents a more general discussion of the atomic many-body problem, designed to direct the interested reader to literature that describes a wider variety of approaches. In the following section we describe the physics of highly charged ions, which is one area of atomic physics where extremely accurate solutions to the many-body problem are avail-

[1]This is the first article of the first issue of a four-issue set devoted to the proceedings of the Workshop on Coupled-Cluster Theory at the Interface of Atomic Physics and Quantum Chemistry, which took place at the Harvard-Smithsonian Center for Astrophysics, August 6–11, 1990.

able, and in which a full QED treatment is required. We start, however, with a discussion of MBPT and give details about the basis-set techniques used to carry out MBPT calculations in atomic physics. The connection of MBPT with a QED treatment based on the S-matrix approach is then described, and an example of a combined MBPT/QED calculation in a many-electron ion is given.

In the next section we briefly describe a second area in which extremely accurate solutions have been found, the few-electron atoms, helium and lithium. We also introduce methods for summing all orders of perturbation theory that are exact for helium and connect them with the Bethe-Salpeter equation. In the following section MBPT is applied to heavy alkalis through third order for energies and matrix elements, and agreement with experiment at the one-percent level is demonstrated. In the final section ''all-orders'' techniques, which sum infinite classes of diagrams, are shown to allow even more accurate determinations, and speculations are presented as to what techniques could lead to tenth-of-a-percent or lower precision.

We make the following comments about terminology and units. Unless otherwise stated, atomic units are used for energies, with 1 a.u. = 1 Hartree = 27.2114 eV. The solution to the Dirac equation with angular momentum κ, magnetic quantum number m, and principal quantum number n is

$$\psi_{n\kappa m}(\vec{r})=\frac{1}{r}\begin{pmatrix} ig_{n\kappa}(r)\chi_{\kappa m}(\Omega_r) \\ f_{n\kappa}(r)\chi_{-\kappa m}(\Omega_r)\end{pmatrix}, \tag{3}$$

where the spherical spinors are defined conventionally. We shall use the term 'structure problem' to refer to the issues involved in solving the nonrelativistic Schrödinger equation, even when the Dirac equation is used, and ''field-theoretic effects'' to refer to the extra physics present in QED, specifically the effect of negative-energy states, retardation of the photon propagator, and radiative corrections. With the exception of the next section, the only atoms considered will be alkali atoms, atoms with a single valence electron outside a closed shell, and helium.

II. OVERVIEW OF THE ATOMIC MANY-BODY PROBLEM

The first application of diagrammatic many-body perturbation theory to atomic physics was made by Kelly (1964). This paper is reprinted in Sinanoglu and Brueckner (1970), which is a good source for the literature before 1970. In particular, early Hartree-Fock calculations and the seminal paper by Goldstone (1957) are included, along with papers treating atoms as a nonuniform electron gas, early work on the four-electron system of beryllium, which we discuss below, and a particularly interesting Green's-function approach by Tolmachev. Three textbooks on the subject of particular note are those of Sobel'man (1972), Cowan (1981), and Lindgren and Morrison (1986).

While the Hartree-Fock method gives a relatively good total energy for an atom, this energy is rarely of experimental interest. Of more direct interest is the energy required to raise a valence electron to an excited state. For these smaller energies the difference between the results of a Hartree-Fock calculation and experiment, defined as *correlation*, is sizable, and techniques for the accurate calculation of correlation, which is of course equivalent to the accurate solution of the Schrödinger equation, must be developed. An important improvement of the Hartree-Fock method is the multiconfigurational Hartree-Fock (MCHF) method (Froese Fischer, 1986) and its relativistic generalization, multiconfigurational Dirac-Fock (MCDF; Desclaux, 1975, 1977; Grant *et al.*, 1980; McKenzie *et al.*, 1980). A textbook discussion of the numerical implementation of HF and MCHF methods is given by Froese Fischer (1977). Computer packages exist for both MCHF and MCDF and are very useful, in particular for obtaining relatively accurate predictions for general atomic states. However, it can be difficult to improve precision systematically: a typical problem is the occurrence of numerical instability when a relatively weak configuration is added. When the orbitals are fixed instead of being allowed to vary, one is dealing with configuration interaction, which will be discussed in a subsequent section. Here we simply note that while not allowing the orbitals to vary eliminates the problem of convergence, the choice of which orbitals to include must be made with care, and as the number of included orbitals increases, extremely computation-intensive calculations result.

While in this review emphasis is put on helium and alkali atoms and ions, an important test case in atomic physics is the neutral beryllium atom. The state of the art, as of 1976, for calculations of this atom, which has strong mixing between the $2s^2$ and $2p^2$ configurations, was summarized by Lindgren and Morrison (1986), who showed a variety of methods to reproduce between 95 and 104 percent of correlation, with the classic configuration-interaction calculation of Bunge (1976) being the most complete. However, to compare this nonrelativistic calculation to experiment, one must include relativistic, QED, and finite-nuclear-mass effects. There has been considerable activity in this field recently, and we refer the interested reader to the papers of Liu and Kelly (1991), Lindroth *et al.* (1992, 1995), and Chung *et al.* (1993).

There are a variety of ways of implementing perturbation theory. Even when the interaction is time independent, time-dependent methods can be useful: as an example, the Goldstone paper used such a method. When we treat QED, where the interactions are in general time dependent, it is natural to use the language of Feynman diagrams. When Feynman diagrams are used, there is an additional integration present over a fourth component of momentum. If this is carried out with Cauchy's theorem, a larger set of terms arises that correspond to time-ordered perturbation theory. In the many-body problem, these terms are represented by Goldstone diagrams. As in the relativistic case, the use

of Feynman diagrams is more compact, although the cost is the presence of an additional integration. Extensive calculations in which the integration is carried out numerically have been performed out by the Novosibirsk group (Dzuba *et al.*, 1986, 1989, 1995), as will be discussed further below. We note also the variants of Goldstone diagrams that automatically include exchange diagrams, known as Brandow diagrams (Brandow, 1967): the use of these substantially reduces the number of time-ordered diagrams that must be considered in a given order.

We next turn to a discussion of the different ways of implementing infinite sums of MBPT diagrams. There are, particularly in quantum chemistry, a great number of different methods, roughly divided along the lines of how many electrons are excited. Almost all accurate methods excite at least two electrons, although we note that excitations of closed-shell atoms can be treated fairly well with the essentially one-electron excitation method of the random phase approximation (RPA; Fetter and Walecka, 1971). The book of Lindgren and Morrison (1986) gives a thorough discussion of the *pair equation*, an equation that sums up two-electron excitations. A particularly powerful and general method is the coupled-cluster method (Bishop and Kummel, 1987; Bartlett, 1991). The all-orders method described later in this review is a linearized form of the coupled-cluster method, though we will describe a nonlinear term in the last section. The method has also been used extensively in chemistry, nuclear physics, and condensed-matter physics.

The Novosibirsk group also sums infinite classes of diagrams, in this case, however, Feynman rather than Goldstone diagrams. Despite the complication of having to carry out an extra integration, they are able to sum a particularly important set of polarization diagrams that incorporate the effect of electron screening (Dzuba *et al.*, 1989). With this method, calculations that agree with experiment somewhat better than the all-orders methods described in this review have been carried out on a number of atoms, notably cesium (Dzuba *et al.*, 1989), thallium (Dzuba *et al.*, 1986), and francium (Dzuba *et al.*, 1995).

The method of quantum Monte Carlo (Ceperley and Mitas, 1996) is beginning to be applied to the atomic many-body problem. However, there is an important problem with a recent application of the method to lithium. One of the highest accuracies claimed for this method was for an oscillator strength of lithium (Barnett *et al.*, 1995). At the time that calculation was presented, the experimental situation (Gaupp *et al.*, 1982) appeared to indicate a discrepancy with theory, which was puzzling because entirely different theoretical techniques were all in agreement. A very-high-accuracy Hylleraas coordinate calculation, along with references to these other theoretical calculations, is given by Yan and Drake (1995). The result of Barnett *et al.* (1995), in contrast, agrees with experiment. However, several experiments have been carried out since (Volz and Schmoranzer, 1996; Carlsson and Sturesson, 1989; McAlexander *et al.*, 1995), all in agreement with non–Monte Carlo theory and in disagreement with the earlier experiment, and it is almost certain that some systematic effect was not accounted for in the older experiment. Until this discrepancy is resolved, we consider the utility of Monte Carlo methods for high-accuracy atomic calculations to be in question and strongly urge new calculations on lithium.

While the treatment of angular momentum for a single valence electron is trivial, it becomes rapidly more complicated as more valence electrons are added. While this is not a fundamental problem, there are two features of atoms with complex spectra that make them less suitable for high-precision work. One is simply the very large number of states and transitions present. For example, the compilation of Fuhr *et al.* (1988) gives information on approximately 2000 allowed transitions in iron. It is complicated to work out even the lowest-order predictions for such a large set of transitions, and since a fair amount of computing is required to go beyond lowest order, as will be discussed below, there is a strong incentive to concentrate on simpler systems with just a few well-measured transitions. In addition, the large number of configurations with similar energies leads to mixing problems similar to, but more severe than, those mentioned in connection with beryllium. We note that the group-theoretic method of orthogonal parameters (Hansen and Judd, 1986) has proven useful for these more complicated systems.

III. THE MANY-BODY PROBLEM FOR HIGHLY CHARGED IONS

One of the most interesting features of the atomic many-body problem is the fact that it is based on our most successful field theory, quantum electrodynamics. This means that even if the structure problem is solved exactly, small deviations from experiment must exist, and these deviations should be calculable. These field-theoretic effects require the full apparatus of QED for their calculation. Given that it was developments in QED that led to the modern form of the many-body problem, it is clear that this theory is in principle powerful enough to deal with both the structure and field-theoretic parts of the problem. However, until recently, most spectroscopic data available for atoms came from neutral atoms, in which the QED corrections are very small, the leading correction being the Lamb shift, which enters in order $Z^4\alpha^3$ atomic units. For transitions between outer electrons, which see a highly screened nuclear charge, the effective Z is of order unity, and the Lamb shift is generally smaller than the uncertainties of the structure problem. There are two situations in which QED corrections are enhanced in heavy atoms. The first is when deeply bound electrons, which are not highly screened, are probed, as is the case in the field of inner-shell x rays, which was one of the first places in which QED effects in many-electron atoms were studied (Johnson and Cheng, 1985). There has been considerable recent progress in this field (Indelicato and Lin-

droth, 1992; Lindroth and Indelicato, 1994). However, more recently a wealth of data on highly stripped ions, with $Z \gg N$, has become available, and in these systems the screening plays a smaller role. For purposes of illustration, we concentrate on sodiumlike platinum, on which precise measurements have been carried out in an electron-beam ion trap (Cowan *et al.*, 1991). We shall demonstrate below that MBPT converges very rapidly for such ions. The basic reason for this rapid convergence is the dominant influence of the nucleus, which forces the electrons into near-hydrogenic orbitals. The repulsive interaction between the electrons can then be treated as a perturbation, although we shall see that with eleven electrons present it is advantageous to build in some of the effects of screening in the lowest-order problem.

A. Relativistic many-body perturbation theory

Because relativistic effects are large in highly charged ions, we generalize the original Hamiltonian of the introduction to $H=H_0+V_C+B$, where

$$H_0=\sum_{i=1}^{N}(\vec{\alpha}_i\cdot\vec{p}_i+\beta_i m)-\sum_{i=1}^{N}\frac{Z(r_i)\alpha}{r_i}, \tag{4}$$

$$V_C=\frac{1}{2}\sum_{i\neq j}\frac{\alpha}{|\vec{r}_i-\vec{r}_j|}, \tag{5}$$

and

$$B=-\frac{\alpha}{2}\sum_{i\neq j}\frac{\vec{\alpha}_i\cdot\vec{\alpha}_j+\vec{\alpha}_i\cdot\hat{r}_{ij}\vec{\alpha}_j\cdot\hat{r}_{ij}}{|\vec{r}_i-\vec{r}_j|}. \tag{6}$$

We have written an r-dependent nuclear charge to account for the finite size of the nucleus, which can give sizable effects for $s_{1/2}$ and $p_{1/2}$ states. In practice, the nucleus is generally modeled with a Fermi distribution. Other distributions, as long as they are chosen to give the same rms radius, give the same answer to a high degree of accuracy. It is straightforward to include nonspherical nuclei. We have also included the instantaneous Breit interaction because it gives a relatively large contribution, entering in order $Z^3\alpha^2$ a.u.

The above Hamiltonian is known to be ill defined (Brown and Ravenhall, 1951) because it does not prohibit transitions to negative-energy states. The problem has been referred to (Sucher, 1980, 1984; see also Mittelman, 1981) as *continuum dissolution*. To address this problem, we add the simple rule that, when carrying out MBPT calculations, negative-energy states are to be excluded from sums over intermediate states. When we introduce the QED formalism, we shall see that this apparently *ad hoc* rule is justified, but that certain relatively small field-theoretic effects involving the negative-energy states enter in a well-defined way.

If H_0 is treated as the lowest-order Hamiltonian, perturbation theory gives the $1/Z$ expansion (Doyle, 1969), in which each succeeding order of perturbation theory is accompanied by a factor of $1/Z$. However, it is advantageous for highly charged ions, and absolutely necessary for neutral atoms, to build in an approximation to the screening of the nuclear charge by the electrons in the lowest-order Hamiltonian. Therefore we rearrange the Hamiltonian into $H=H_0+H_I+B$, where now

$$H_0=\sum_{i=1}^{N}(\vec{\alpha}_i\cdot\vec{p}_i+\beta_i m)-\sum_{i=1}^{N}\frac{Z(r_i)\alpha}{r_i}+\sum_{i=1}^{N}U(r_i) \tag{7}$$

and

$$H_I=\frac{1}{2}\sum_{i\neq j}\frac{\alpha}{|\vec{r}_i-\vec{r}_j|}-\sum_{i=1}^{N}U(r_i), \tag{8}$$

where $U(r)$ is designed to account for the presence of the other electrons and will be discussed further below. We now wish to apply perturbation theory in the first three orders for alkali-like systems.

Because this perturbation theory, particularly its diagrammatic representation, is very well known, we will not rederive the formulas here: a standard reference for MBPT in atomic physics is the book of Lindgren and Morrison (1986). Because of the separation of the closed-shell core from excited states, we introduce the notation that $a,b,c,\ldots$ indicate summations over the core, and $m,n,r,\ldots$ summations over excited states. We reserve v and w for the valence states (which are, unless otherwise indicated, included in summations over excited states). When all states are summed we use the letters $i,j,k,\ldots$. For sodiumlike platinum the core states consist of the $1s_{1/2}$, $2s_{1/2}$, $2p_{1/2}$, and $2p_{3/2}$ states, and the valence states will be the $3s_{1/2}$ and $3p_{3/2}$ states. Note that in this highly relativistic system the splitting between the $3p_{1/2}$ and $3p_{3/2}$ states is very large, and that j-j coupling is the appropriate coupling scheme. The second-quantized representation of a valence state is

$$|\Psi_v\rangle=a_v^\dagger|0_C\rangle, \tag{9}$$

where

$$|0_C\rangle=\prod_{i=1}^{N-1}a_i^\dagger|0\rangle \tag{10}$$

represents the closed-shell core. The second quantized representation of H_I is

$$H_I=\frac{1}{2}\sum_{ijkl}g_{ijkl}a_i^\dagger a_j^\dagger a_l a_k-\sum_{ij}U_{ij}a_i^\dagger a_j. \tag{11}$$

Here we have introduced the Coulomb integral

$$g_{ijkl}\equiv\alpha\int\frac{d^3r\,d^3r'}{|\vec{r}-\vec{r}'|}\overline{\psi}_i(\vec{r})\gamma_0\psi_k(\vec{r})\overline{\psi}_j(\vec{r}')\gamma_0\psi_l(\vec{r}') \tag{12}$$

and matrix elements of the model potential

$$U_{ij}=\int d^3r\,\overline{\psi}_i(\vec{r})\gamma_0 U(r)\psi_j(\vec{r}). \tag{13}$$

We have written $\overline{\psi}\gamma_0$ rather than the equivalent $\psi^\dagger$ in the above to emphasize the connection with field theory: the Coulomb matrix elements correspond to exchange of a Coulomb photon in Coulomb gauge, and the model potential is the fourth component of a four-vector.

B. Choice of potentials

The choice of the model potential is in principle arbitrary, but in practice one clearly wants to have a lowest-order solution that gives a reasonable approximation to energies and matrix elements. It is possible to devise model potentials with a number of parameters that can be fit to an accuracy at the percent level (Johnson, Guo, *et al.*, 1986). While such potentials can be useful, for the purposes of precision work it is actually better to use a potential that gives less accurate starting values. This is because model potentials are devised to give extremely accurate lowest-order answers, but higher orders in perturbation theory will almost always give less accurate answers. In practice, the Hartree-Fock potential provides a good starting point. It also has the advantage that many terms in MBPT vanish automatically when it is chosen. However, because it is a nonlocal potential, the connection with QED cannot be made as directly as with local potentials. The nonlocality also leads to a loss of gauge invariance: energy shifts from one-photon exchange are different in Coulomb and Feynman gauge when the Hartree-Fock potential is used (Mann and Johnson, 1971; Gorceix and Indelicato, 1988; Lindgren, 1990; Chen, 1993). Thus it is useful to introduce two potentials that are determined self-consistently in a manner similar to Hartree Fock, but that are local. The first of these we refer to as the core-Hartree potential. It is given by

$$U_{\rm CH}(r)=\sum_a\ (2j_a+1)y_0(a,a;r) \tag{14}$$

where

$$y_0(a,a;r)=\alpha\int_0^\infty dr'\,\frac{1}{r_>}[g_a^2(r')+f_a^2(r')]. \tag{15}$$

with $r_>=\max(r,r')$. As $r\to\infty$, $y_0\to\alpha/r$, so that the nuclear charge is asymptotically screened by the number of electrons in the core, as is physically reasonable for alkali systems. The wave functions $g_a(r)$ and $f_a(r)$ are determined self-consistently. The second potential, which we refer to as the modified core-Hartree potential, is

$$U_{\rm MCH}(r)=\sum_a\ (2j_a+1)y_0(a,a;r)-y_0(a_0,a_0;r), \tag{16}$$

where a_0 is the least strongly bound core state, $2p_{3/2}$ in the present case. Its asymptotic charge is $Z-N+1$, which is most appropriate for closed-shell systems. The final potential we shall consider is simply the nuclear Coulomb potential, in which screening is treated entirely perturbatively. Many-body perturbation theory with this potential in the nonrelativistic limit, gives the previously mentioned $1/Z$ expansion, in which the nth order of perturbation theory gives a contribution that scales as $Z^{(2-n)}$ a.u. For high Z we shall show that high accuracy results from including MBPT through second order regardless of the starting potential.

The first two orders of MBPT give the standard results

$$E^{(0)}=\epsilon_v+\sum_a\ \epsilon_a \tag{17}$$

and

$$E^{(1)}=(V_{\rm HF}-U)_{vv}+\sum_a\ (\tfrac{1}{2}V_{\rm HF}-U)_{aa}\,. \tag{18}$$

We have introduced here the nonlocal Hartree-Fock potential $V_{\rm HF}$ defined as

$$(V_{\rm HF})_{ij}=\sum_a\ \tilde{g}_{iaja} \tag{19}$$

where

$$\tilde{g}_{ijkl}\equiv g_{ijkl}-g_{ijlk}\,. \tag{20}$$

We note that, if the Hartree-Fock potential is chosen, the valence part of the first-order energy vanishes.

Continuing to the second-order energy, we divide into $E^{(2)}=E^{(2)}_{\rm core}+E^{(2)}_{\rm val}$, with

$$E^{(2)}_{\rm core}=\frac{1}{2}\sum_{abmn}\frac{g_{abmn}\tilde{g}_{mnab}}{\epsilon_{ab}-\epsilon_{mn}}+\sum_{am}\frac{X_{am}X_{ma}}{\epsilon_a-\epsilon_m} \tag{21}$$

and

$$E^{(2)}_{\rm val}=\sum_{amn}\frac{g_{vamn}\tilde{g}_{mnva}}{\epsilon_{va}-\epsilon_{mn}}-\sum_{abm}\frac{g_{abmv}\tilde{g}_{mvab}}{\epsilon_{ab}-\epsilon_{mv}} +\sum_{am}\left[\frac{X_{am}\tilde{g}_{mvav}}{\epsilon_a-\epsilon_m}+\frac{X_{ma}\tilde{g}_{vavm}}{\epsilon_a-\epsilon_m}\right]-\sum_{i\neq v}\frac{X_{vi}X_{iv}}{\epsilon_i-\epsilon_v}\,, \tag{22}$$

where we have introduced the notations $X=V_{\rm HF}-U$ and $\epsilon_{ab\cdots z}=\epsilon_a+\epsilon_b+\ \ldots\ +\epsilon_z$. The problems with continuum dissolution first show up in this order. If the restriction of summing over only positive-energy states were not in place, vanishing energy denominators could occur in sums involving two excited states m and n. Specifically, the first term of $E^{(2)}_{\rm core}$ involves the denominator $\epsilon_a+\epsilon_b-\epsilon_m-\epsilon_n$. If n is a negative-energy state with energy $-mc^2-\Delta$, the state m with energy $\epsilon_a+\epsilon_b+mc^2+\Delta$ will lead to a vanishing energy denominator. We shall see later that when QED is fully implemented such terms do not occur. However, the state where both m and n are negative-energy states will enter as a QED correction, but with a sign change.

The accurate evaluation of terms involving a single sum over states can be carried out with differential-equation techniques. However, the double summations present in the second-order energy, while they can also be treated with differential-equation methods (McKoy and Winter, 1968; Musher and Shulman, 1968; Lindroth, 1988), are better treated with the numerical technique of finite basis sets, which we now briefly describe.

C. Finite basis sets

The numerical evaluation of the second-order energy can be carried out with high accuracy with the technique

of finite basis sets. The sums over excited states involve both an infinite summation over bound states and an integration over the continuum, which are awkward to deal with, especially when multiple sums are present. The basic idea of finite basis sets is to replace this summation and integration with a single finite summation over a *pseudospectrum*. There are a variety of ways of doing this. Examples of the use of nonrelativistic basis sets can be found in Chang and Tang (1991), Froese Fisher *et al.* (1992), and Hansen *et al.* (1993), and of relativistic basis sets in Johnson and Sapirstein (1986), Bottcher and Strayer (1987), Salomonson and Oster (1989a, 1989b, 1990), and Eliav *et al.* (1996a, 1996b). Relativistic basis sets have recently been discussed in detail by Grant (1996). The approach described here is taken from a recent review (Sapirstein and Johnson, 1996).

The first step in forming a finite basis set is to confine the atom in a cavity of radius R, which discretizes the continuum and limits the number of bound states. The radius is chosen sufficiently large so as not to distort the states one is dealing with: typically a value of 40 a.u. is chosen. The implementation of this boundary condition requires some care in the relativistic problem: if one attempts to confine the electron by making the fourth component of a potential go to infinity for $r>R$, the Klein paradox will lead to oscillatory solutions. The same problem occurs when hadrons are treated as bound states of quarks and is solved by making the mass become large for $r>R$, as in the MIT bag model (Chodos *et al.*, 1974). This leads to the boundary condition $P(R)=Q(R)$ in the representation of the wave function

$$\psi_{n\kappa m}(\vec{r})=\frac{1}{r}\begin{pmatrix} iP_{n\kappa}(r)\chi_{\kappa m}(\Omega_r) \\ Q_{n\kappa}(r)\chi_{-\kappa m}(\Omega_r)\end{pmatrix}. \tag{23}$$

At this point there is a denumerable infinity of states. The next step is to turn this into a finite number. One way of doing this is to set up the radial Dirac equation on a lattice of n points and use an approximation for the derivative, which leads to an $n\times n$ eigenvalue problem. This is the method used by the Goteborg group (Salomonson and Oster; 1989a, 1989b, 1990). Here we adopt a local approach by first forming the action whose variation leads to the radial Dirac equation,

$$\begin{aligned} S=\frac{1}{2}\int_0^R dr\Big[&\frac{1}{\alpha}P_\kappa(r)\left(\frac{d}{dr}-\frac{\kappa}{r}\right)Q_\kappa(r)-\frac{1}{\alpha}Q_\kappa(r) \\ &\times\left(\frac{d}{dr}+\frac{\kappa}{r}\right)P_\kappa(r)-\frac{Z}{r}[P_\kappa^2(r)+Q_\kappa^2(r)] \\ &-\frac{2}{\alpha^2}Q_\kappa^2(r)\Big]-\frac{1}{2}\epsilon\int_0^R dr[P_\kappa^2(r)+Q_\kappa^2(r)] \\ &+S_{\text{boundary}}. \end{aligned} \tag{24}$$

The boundary conditions are implemented through the last term, which is

$$S_{\text{boundary}}(\kappa<0)=\frac{1}{4\alpha}[P_\kappa^2(R)-Q_\kappa^2(R)]+\frac{1}{2\alpha}P_\kappa^2(0) -\frac{1}{2\alpha}P_\kappa(0)Q_\kappa(0) \tag{25}$$

and

$$S_{\text{boundary}}(\kappa>0)=\frac{1}{4\alpha}[P_\kappa^2(R)-Q_\kappa^2(R)]+\frac{1}{\alpha^2}P_\kappa^2(0) -\frac{1}{2\alpha}P_\kappa(0)Q_\kappa(0). \tag{26}$$

The surface terms from partial integration taken together with the variation of S_{boundary} force $P_\kappa(R)=Q_\kappa(R)$ and $P_\kappa(0)=0$. The latter constraint comes from the term in S_{boundary} which involves $P_\kappa(0)^2$. The larger constant multiplying this term for the case $\kappa>0$ is chosen empirically in order to prevent the occurrence of spurious states. Spurious states are parts of the pseudospectrum with nonphysical energies that lie in the bound-state spectrum, typically having the lowest bound-state energy. It is important to note that this is not a fundamental problem: these states oscillate rapidly and play a negligible role in sum-over-states calculations. However, it is easier to work with a spline basis set if the first members directly correspond to physical bound states. In the rare cases when the above choice of boundary conditions allows such a state, it is simply moved to the end of the set.

A pseudospectrum can now be formed by expanding $P(r)$ and $Q(r)$ in terms of a set of functions $B_i(r)$,

$$P(r)=\sum_i^n p_i B_i(r) \tag{27}$$

and

$$Q(r)=\sum_i^n q_i B_i(r), \tag{28}$$

where we leave the precise form of these functions arbitrary at first. Inserting this form into the above action then leads to a quadratic form in p and q. By then varying this form with respect to these coefficients, we obtain a $(2n)\times(2n)$ symmetric eigenvalue equation. When this is solved, n positive-energy eigenstates and n negative-energy eigenstates result. The first few eigenvalues and eigenvectors of the pseudospectrum agree accurately with the corresponding bound-state spectrum, but as the principal quantum number increases the finite cavity radius comes into play and makes the number of bound states finite. The remainder of the pseudospectrum mocks up the effect of the continuum, which plays a significant role in atomic calculations. As an example of how a pseudospectrum works, we show in the nonrelativistic case how the calculation of the second-order Stark effect in ground-state hydrogen is done with a finite basis set. In this case we need to evaluate

$$\Delta E^{(2)}=\sum_{n\neq 0}\frac{\langle 0|V|n\rangle\langle n|V|0\rangle}{E_n-E_0}, \tag{29}$$

TABLE I. The p-state basis-set energies E_n and the corresponding contributions Δ_n to second-order Stark energy in units of $E^2a_0^3$; F_n is the accumulated sum of n terms.

n	E_n	Δ_n	F_n	n	E_n	Δ_n	F_n
1	−0.125000000	−1.479810556	−1.479810556	12	0.572938252	−0.027136410	−2.239070250
2	−0.055554769	−0.200265484	−1.680076040	13	1.000339413	−0.005524789	−2.244595039
3	−0.030709894	−0.074730694	−1.754806734	14	1.081844500	−0.003290999	−2.247886038
4	−0.012210968	−0.074847349	−1.829654083	15	1.858618191	−0.001790416	−2.249676454
5	0.013028340	−0.080520638	−1.910174721	16	3.294396540	−0.000282167	−2.249958621
6	0.045678279	−0.075118292	−1.985293013	17	5.782998725	−0.000036648	−2.249995269
7	0.085332699	−0.064650213	−2.049943226	18	10.06435005	−0.000004226	−2.249999495
8	0.132033682	−0.050887383	−2.100830609	19	17.39480449	−0.000000453	−2.249999948
9	0.187982878	−0.050069613	−2.150900222	20	29.90376820	−0.000000046	−2.249999994
10	0.274396937	−0.02629715	−2.177197376	21	51.19778804	−0.000000005	−2.249999999
11	0.340020874	−0.034736465	−2.211933841	22	87.38274723	−0.000000000	−2.249999999

with $V=eEz$. This summation can be evaluated analytically by replacing the sum over n with the solution of a differential equation (Schiff, 1968), with the result, in units of $E^2a_0^3$, of $-9/4$. With finite basis sets we instead directly carry out the sum over n in terms of a pseudospectrum of p states. With a basis set of size 50, the individual and accumulated contributions to the sum are shown in Table I.

This procedure should be contrasted with the direct evaluation of the sum in terms of an infinite sum over the bound states and an integration over the continuum: in the present case, only the first four states are bound, and the remaining states are unbound. However, the spline basis set is seen to be effectively complete to ten digits, and greater accuracy can be obtained by using a larger basis set.

The exact choice of basis functions $B_i(r)$ is in principle arbitrary: popular choices in atomic and molecular physics are Slater and Gaussian functions. The table above and subsequent results presented in this review use basis sets based on B splines (DeBoor, 1978), polynomials that vanish everywhere except in a limited range. One advantage of these functions is that the matrices that enter the eigenvalue problem described above are automatically banded, which allows very large basis sets to be formed without problems of linear dependence. A typical basis set used in the atomic correlation calculations described here will consist of 40 eigenfunctions for each value of angular momentum and will be accurate to about five digits. If greater accuracy is desired, 50 or 60 eigenfunctions will be used. To calculate atomic parity nonconservation, which is particularly difficult owing to the need to describe the atomic wave function accurately at both small and large scales, 70 are required.

D. Angular momentum

Because of the spherical symmetry of atomic physics, angular momentum techniques play a central role in the many-body problem. The basic building block of many-body perturbation theory, g_{ijkl}, can be reduced to a summation over two-dimensional radial integrals by carrying out a partial-wave expansion of the $|\vec{r}-\vec{r}'|$ denominator,

$$g_{ijkl}\equiv\alpha\int d^3rd^3r'\sum_{lm}\frac{4\pi}{2l+1}\frac{r_<^l}{r_>^{l+1}} \times Y_{lm}(\Omega)Y_{lm}^*(\Omega')\overline{\psi}_i(\vec{r})\gamma_0\psi_k(\vec{r})\overline{\psi}_j(\vec{r}')\gamma_0\psi_l(\vec{r}'). \tag{30}$$

Putting in the explicit form of the wave functions allows the angle integrations to be done analytically, leading to the expansion

$$g_{ijkl}=\sum_{lm}(-1)^{j_i+j_j-\mu_j-\mu_k}C_l(ik)C_l(jl)R_l(ijkl) \times\begin{pmatrix} l & j_i & j_k \\ m & \mu_i & -\mu_k\end{pmatrix}\begin{pmatrix} l & j_l & j_j \\ m & \mu_l & -\mu_j\end{pmatrix}, \tag{31}$$

where

$$R_l(ijkl)=\int dr\int dr'\frac{r_<^l}{r_>^{l+1}}[g_i(r)g_k(r)+f_i(r)f_k(r)] \times[g_j(r')g_l(r')+f_j(r')f_l(r')] \tag{32}$$

and

$$C_l(ba)=(-1)^{(j_b+1/2)}\sqrt{(2j_a+1)(2j_b+1)} \times\begin{pmatrix} l & j_b & j_a \\ 0 & \mu_b & -\mu_a\end{pmatrix}\Pi(l_a,l_b,l), \tag{33}$$

where the parity factor Π is 1 if l_a+l_b+l is even and 0 otherwise.

When a sum over states is present, it is broken up as

$$\sum_n=\sum_{\kappa_n=-\infty}^{\infty}\sum_{\mu=-j_n}^{j_n}\sum_{n=1}^{N}, \tag{34}$$

where κ is the angular momentum, μ the magnetic quantum number, and n the principal quantum number, which is now a finite sum because of our use of basis sets. The sum over μ can always be carried out analyti-

TABLE II. $E^{(2)}(l)$ for He with a (50,9) spline basis set in a cavity radius $R = 40$ a.u.

l	$E^{(2)}_{\rm NR}(l)$	l	$E^{(2)}_{\rm NR}(l)$
0	−0.12535611	6	−0.00009556
1	−0.02649241	7	−0.00005422
2	−0.00390465	8	−0.00003298
3	−0.00107694	9	−0.00002119
4	−0.00040562	10	−0.00001424
5	−0.00018467	11−∞	−0.00004357
		Sum	−0.15768216

cally, but the sum over κ is in general unbounded. Thus, for example, the angular reduction of the second-order energy for ground-state helium results in

$$E^{(2)}=\sum_{l=0}^{\infty}\frac{l}{(2l+1)^3}\sum_{mn}\left.\frac{R_l(mn1s1s)^2}{2\epsilon_{1s}-\epsilon_m-\epsilon_n}\right|_{\kappa=l} +\sum_{l=0}^{\infty}\frac{l+1}{(2l+1)^3}\sum_{mn}\left.\frac{R_l(mn1s1s)^2}{2\epsilon_{1s}-\epsilon_m-\epsilon_n}\right|_{\kappa=-l-1}. \tag{35}$$

While the sum over l cannot of course be directly extended to infinity, the bulk of the contribution is picked up by including in the basis set all states that are associated with low values of l, as illustrated in Table II.

For high-accuracy work, the remaining part of the partial-wave summation can be included by noting the behavior of the high-l terms: typically a $1/l^4$ behavior has set in by around $l=8$, which allows the extrapolation of the sum to infinity, as done in Table II. (Some relativistic effects converge only as $1/l^2$, which requires inclusion of more partial waves.) In the case of helium, Schwartz (1962) has shown that the exact high-l behavior goes as $1/(l+\frac{1}{2})^4$, which follows from considerations of the cusp of the helium wave function. Ground-state helium is simpler than most cases in that only two values of κ can contribute for a given l. In general the number of allowed values increases rapidly, and increasing the maximum value of l rapidly increases the amount of computation required. This fact is one of the main limitations on the accuracy when evaluating MBPT expressions, as there is always some uncertainty in the extrapolation to infinity.

E. Many-body perturbation theory applied to sodiumlike platinum

The high-accuracy electron-beam ion trap experiment on sodiumlike platinum (Cowan *et al.*, 1991) mentioned above measures the transition between the $3p_{3/2}$ and $3s_{1/2}$ states. This transition is in the x-ray region and corresponds to the energy 653.44(7) eV. We shall see that MBPT gives an answer about 1 percent higher than this measurement, which is accounted for almost entirely by one-loop radiative corrections. To study these corrections it is crucial to solve the MBPT part of the problem to high accuracy. This is the same issue as mentioned in connection with parity nonconservation in neutral atoms: to study relatively small radiative corrections in atoms, the structure problem must be solved to well below the level at which the radiative corrections enter. The problem of reliably determining the accuracy of MBPT when calculated to a given order is in general very challenging in the case of neutral atoms, as will be discussed later. However, the scaling of the nth order of MBPT with the nuclear charge in the $1/Z$ expansion, Z^{2-n} a.u., suggests that third- and higher-order contributions will be strongly suppressed in highly charged ions. To test this in practice, we shall in this section calculate energy levels of sodiumlike platinum using four different potentials and include all contributions through second order. In addition, we shall explicitly include the third-order energy for the Hartree-Fock case and show that it is much smaller than the field-theoretic effects.

TABLE III. Behavior of many-body perturbation theory for different potentials: units eV.

Order	HF	CH	MCH	Coulomb
0	659.63	649.40	647.47	626.73
0+1	659.63	659.44	659.81	674.95
0+1+2	659.56	659.59	659.57	659.72

With the basis-set methods described above, it is straightforward to calculate the second-order energy correction. Note that because what is measured is a transition between two valence states, the contributions from the energy of the core cancel out and are thus not included in the calculation. Neglecting the Breit interaction, we find that the four potentials discussed above behave as in Table III.

We make the following comments about the behavior of MBPT in this case. First, the Hartree-Fock potential behaves particularly well, having no first-order correction and a relatively small correlation correction. The core-Hartree and modified core-Hartree potentials start out in lowest order differing by about 10 eV, but this is reduced to a few tenths of an eV after the first-order corrections are included. The Coulomb potential, however, because it entirely leaves out screening, starts out below the Hartree-Fock result by 50 eV, and first-order perturbation theory overcompensates, taking it to 15 eV above. However, upon inclusion of the second-order energy, the potentials that include screening all agree to within a few hundredths of an eV, and even the Coulomb potential has come into agreement at the tenth-of-an-eV level. The third-order energy has only been evaluated in the Hartree-Fock case and contributes a negligible −0.0002 eV. Thus it is reasonable to assume that the "structure" part of the calculation is reliable at below the tenth-of-an-eV level.

Before comparing with experiment, two other effects must be included. The first is the instantaneous Breit interaction along with MBPT corrections to it. The second is the finite mass of the nucleus (the finite size is incorporated in the Coulomb calculation), which gives

rise to reduced mass and mass-polarization effects. These change the above answer only slightly, and the final result for the Hartree-Fock potential for this transition is

$$E_{3p_{3/2}} - E_{3s_{1/2}} = 659.50 \text{ eV}. \tag{36}$$

There is simply no untreated term in the structure problem as we have defined it that can account for the 6.1-eV discrepancy of this result with experiment. The explanation is of course quantum electrodynamics (QED), as the Lamb shift is relatively large in highly charged ions. It is perhaps fortunate that such large corrections did not have to be dealt with when the Schrödinger equation was introduced. Discrepancies at the percent level that could only be understood with QED, for which calculations only became practical 25 years after the equation was first written down, could have interfered with the general acceptance of this supremely useful equation.[2]

F. Quantum electrodynamic treatment of the many-body problem

If one is concerned with applying many-body perturbation theory to a given order to atoms or ions, the relation to quantum electrodynamics is quite simple in principle: one simply has to use Furry representation QED (Furry, 1951) with the external potential chosen to be the same as that used in the lowest-order Hamiltonian that defines the MBPT expansion. Of course, if it is not possible to apply MBPT to a sufficiently high order to reduce the wave-function uncertainty below the size of QED effects, this is of academic interest only. The question of how to integrate QED with more powerful techniques that solve the many-body problem with high precision is an open one; however, in general such techniques are not yet in existence for most neutral atoms. An exception is helium, and we shall describe how QED effects are calculated in that system in the next section. However, for highly charged ions MBPT does converge rapidly, and Furry representation QED provides a completely consistent framework for the treatment of both the structure problem and field-theoretic effects. In this section we describe the set of one- and two-photon diagrams that arise in a QED treatment and how they relate to the MBPT described above, which will allow for the precise definition of the field-theoretic effects.

Furry representation is similar to the interaction representation, with the difference that the free Hamiltonian incorporates the nuclear Coulomb field as an external classical field. However, there is nothing to keep one from extending the representation to modify that field to include some effects of screening. In this extension the Hamiltonian of QED is broken into $H = H_0 + H_I$, where

$$H_0 = \int d^3x\, \psi^\dagger(x) \left[\vec{\alpha}\cdot\vec{p} + \beta m - \frac{Z\alpha}{|\vec{x}|} + U(|\vec{x}|) \right] \psi(x) \tag{37}$$

and

$$\begin{aligned} H_I = &- \int d^3x\, \psi^\dagger(x) U(|\vec{x}|) \psi(x) \\ &- e \int d^3x\, \psi^\dagger(x) \vec{\alpha}\cdot\vec{A}(x) \psi(x) \\ &+ \frac{\alpha}{2} \int \frac{d^3x\, d^3x'}{|\vec{x}-\vec{x}'|} \psi^\dagger(x) \psi(x) \psi^\dagger(x') \psi(x'). \end{aligned} \tag{38}$$

If $U = 0$, one is dealing with the original Furry representation, but if one chooses this potential to be a local potential such as the core-Hartree or modified core-Hartree discussed above, this approach to QED will build in some screening and will lead to a close connection with the MBPT based on the potential. The representation is reached by making a unitary transformation on the Schrödinger-picture wave function $|\psi_S\rangle$ to an interaction-picture wave function $|\psi_I\rangle$,

$$|\psi_I\rangle = e^{iH_0 t} |\psi_S\rangle. \tag{39}$$

The usual interaction representation is reproduced when H_0 consists of the free Hamiltonian, and the Furry representation comes from incorporating the nuclear Coulomb field into H_0, but the formalism is clearly general enough to encompass the above breakup of the QED Hamiltonian. $|\psi_I\rangle$ satisfies

$$i\frac{\partial}{\partial t} |\psi_I\rangle = e^{iH_0 t} [H - H_0] e^{-iH_0 t} |\psi_I\rangle \equiv \hat{H}_I |\psi_I\rangle. \tag{40}$$

We construct a perturbation theory to relate Feynman diagrams to energy shifts with Sucher's extension (Sucher, 1957) of the Gell-Mann–Low (1951) formalism. In this approach an adiabatic damping factor is multiplied into H_I,

$$H = H_0 + e^{-\epsilon|t|} H_I. \tag{41}$$

Rather than evolving the wave function at large negative times (at which point it is essentially identical with the lowest-order MBPT wave function) to $t = 0$, Sucher's extension continues the evolution to large positive times and leads to an ϵ-dependent S matrix, defined by

$$|\psi_I(\infty)\rangle \equiv S_\epsilon(\infty, -\infty) |\psi_I(-\infty)\rangle. \tag{42}$$

Energy shifts can now be calculated with the formula

$$\Delta E = \frac{i\epsilon}{2} \lim_{\epsilon\to 0} \lim_{\lambda\to 1} \frac{\partial}{\partial\lambda} \ln\langle S_{\epsilon,\lambda}\rangle, \tag{43}$$

where we have slightly generalized the S matrix to

$$S_{\epsilon,\lambda} = T(e^{-i\lambda\int dx_0 H_I(x_0) e^{-\epsilon|x_0|}}). \tag{44}$$

Expanding S leads to expressions that can be represented as Feynman diagrams, though the conservation

[2]We recall that Schrödinger was supposedly held back for a while from publishing his nonrelativistic equation because he started from the Klein-Gordon equation, which did not properly account for hydrogen fine structure. A discussion of the evidence that this actually happened is given by Kragh (1982).

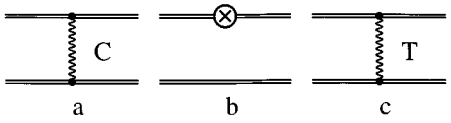

FIG. 1. Feynman diagrams corresponding to the first-order energy.

of the fourth component of momentum at vertices, which is exact when dealing with Feynman diagrams for free particles, is here enforced by factors involving the small parameter ϵ that act as delta functions in the limit $\epsilon \rightarrow 0$. We first consider the Feynman diagrams of Fig. 1 that involve one photon or one screening counterterm for the case of an alkali-like ion. When the photon exchanged is a Coulomb photon [Fig. 1(a)] or when a single screening counterterm is involved [Fig. 1(b)], it is straightforward to show that the associated energy shift is precisely the MBPT formula for $E^{(1)}$. However, a difference arises when the exchanged photon is a transverse one, as in Fig. 1(c). In this case, the fact that energy flows through the photon line when exchange is considered modifies a term in Eq. (6) with, say, $i=1$ and $j=2$, to

$$B_{12}=-\alpha\left[\vec{\alpha}_1\cdot\vec{\alpha}_2\frac{e^{i\omega r_{12}}}{r_{12}}-\vec{\alpha}_1\cdot\vec{\nabla}_1\vec{\alpha}_2\cdot\vec{\nabla}_2\frac{(e^{i\omega r_{12}}-1)}{\omega^2 r_{12}}\right], \tag{45}$$

where ω is the absolute value of the energy flowing through the photon line. Only if the limit $\omega \rightarrow 0$ is taken is the instantaneous Breit interaction that we have used to define the structure problem reproduced. The difference is the first field-theoretic effect we encounter: power counting arguments show that its imaginary part has the leading order $Z^4\alpha^3$ a.u. and the real part $Z^5\alpha^4$ a.u. The former is of the order of the Lamb shift, but is imaginary and contributes only to the decay rate, as will be discussed further in connection with the self-energy diagram below. The latter is an easily seen effect in this system because of the high power of Z, and for the ion we are considering amounts to -0.74 eV. In practical calculations of one-transverse-photon exchange, the division between structure and field-theoretic effects we have been using is often not made, since the calculation of the exact effect is very simple.

The other one-photon diagrams do not have an MBPT counterpart and are pure field-theoretic effects. They are the self-energy and vacuum polarization graphs of Figs. 2(a) and 2(b). At high Z they must be

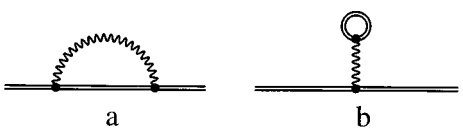

FIG. 2. One-loop radiative corrections.

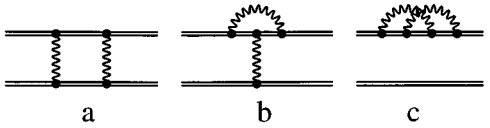

FIG. 3. Representative two-photon Feynman diagrams.

treated in an exact manner, as opposed to the expansion in $Z\alpha$ that is generally applied to low-Z systems. Specifically, the Lamb shift can be parametrized as

$$\Delta E=\frac{Z^4\alpha^3}{n^3\pi}F_n(Z\alpha), \tag{46}$$

where at low Z one can expand

$$F_n(Z\alpha)=A_{40}+A_{41}\ln(Z\alpha)^{-2}+A_{50}Z\alpha+\cdots. \tag{47}$$

For high Z, the perturbation expansion can be shown to completely break down in the sense that including the next higher order can actually change the sign of F_n, and an exact approach is required. Extremely-high-accuracy evaluations of this function for the point-Coulomb case have been carried out by Mohr and collaborators (Mohr, 1992; Mohr and Kim, 1992), and recently high-accuracy techniques for the evaluation of the non-Coulomb case have been introduced (Blundell and Snyderman, 1991; Persson *et al.*, 1993; Cheng *et al.*, 1993). The self-energy part of the Lamb shift has an imaginary part that accounts for one-photon decays of excited states into lower energy states. It would appear that the ground state of sodiumlike platinum would decay because of this, as the $3s$ self-energy has an imaginary part associated with decay to $2p$ states. The stability of the state is accounted for by the imaginary parts of one-photon exchange discussed above, which exactly cancel the imaginary part of the self-energy. This is of course a manifestation of the exclusion principle, which is built into the QED formalism. When excited states are considered or a vacancy is created in the core, the cancellation is incomplete, and a nonvanishing decay rate results.

The results for the self-energy and vacuum polarization for the core-Hartree potential are -6.81 eV and 1.42 eV, respectively. Including the frequency-dependent Breit term, we end up with a prediction of -6.13 eV, almost exactly the field-theoretic effect inferred from the comparison of MBPT and experiment. Note that in the case of the Coulomb potential field-theoretic effects amount to -7.0 eV, so that significant screening is present.

A number of interesting issues are raised by the two-photon diagrams, in which the field-theoretic effects are unfortunately relatively small. Representative graphs are shown in Fig. 3. The first has to do with two-Coulomb photon exchange. For the ground state of helium, the diagram of Fig. 3(a) can be shown (Sapirstein, 1989) to correspond to the integral

$$\Delta E=\frac{i}{2}\sum_{abmn}{}'\int\frac{dk_0}{2\pi}\times\frac{g_{abmn}\tilde{g}_{mnab}}{[\epsilon_a-k_0-\epsilon_m(1-i\delta)][\epsilon_a+k_0-\epsilon_n(1-i\delta)]}. \tag{48}$$

The prime indicates that the state $m=n=1s$ is excluded. Because this is a quantum electrodynamics calculation, the negative-energy-state part of the propagators is present. By applying Cauchy's theorem to the above, one can see that the integral has poles on the same side of the axis when one state is positive energy and the other negative energy, and thus such terms do not contribute. Specifically, carrying out the k_0 integration leads to

$$\Delta E=\frac{1}{2}\sum_{abmn}{}'\frac{g_{abmn}\tilde{g}_{mnab}}{2\epsilon_a-\epsilon_m-\epsilon_n}F_{mn} \tag{49}$$

with

$$F_{++}=-F_{--}=1;F_{+-}=F_{-+}=0. \tag{50}$$

The term with both states of positive energy can be shown to be equivalent to Eq. (21) and is entirely part of the structure problem. However, the term with both states of negative energy was defined to be a field-theoretic effect: power counting arguments show it to enter in order $1/Z$ of the leading Lamb shift. As an example of the relative importance of the two terms, at $Z=50$, the structure part of the graph contributes -0.17301 a.u., while the field-theoretic effect is -0.00017 a.u. The vertex diagrams of Fig. 3(b) also enter in order $Z^3\alpha^3$ a.u. Corrections of this order can be thought of as screening corrections to the Lamb shift, as the phenomenological change $Z\rightarrow Z-\sigma$ changes Z^4 to $Z^4-4Z^3\sigma$, with the second term being of the order of the field-theoretic effects just discussed.

The last set of two-photon diagrams is associated with the two-loop Lamb shift: a representative diagram is shown in Fig. 3(c). The two-loop Lamb shift contributes starting in order $(Z\alpha)^4$ a.u. There is at present considerable interest in the evaluation of the entire set of two-photon diagrams for highly charged ions. Rather than discuss this interesting field further, we simply emphasize the point that this branch of many-body physics is becoming a subfield of quantum electrodynamics, in the sense that evaluation of a well-defined set of Feynman diagrams provides an accurate and unambiguous theoretical prediction. The fact that many electrons are present is accounted for automatically, as would be expected of an intrinsically many-body mathematical formalism such as quantum field theory. However, the great bulk of atomic spectroscopic data has to do with neutral or near-neutral atoms, so we now turn to a discussion of the issues involved in the accurate calculation of these systems, first in helium and lithium, and then in the heavier alkalis.

IV. FEW-BODY ATOMS

Just as the deuteron and triton play special roles in nuclear physics because of the relative simplicity of the many-body problem, so helium, and to a lesser extent lithium, play a special role in atomic physics. The first accurate solutions to the helium problem by Hylleraas (1928, 1929) played an important role in early quantum mechanics, since, unlike the case with hydrogen, this was a problem that the old quantum theory failed in. With modern techniques, while the Schrödinger equation for helium cannot be solved analytically, it can be solved for many states to accuracies well under experimental uncertainty, and for lithium to the nano-Hartree level. As with highly charged ions, differences with experiment are clearly seen that are attributable to relativistic and QED effects. The difference is that the effects are much smaller. At the same time extremely accurate experiments coupled with theory allow the study of these effects, though not quite at the level afforded by hydrogenic systems. Because the variational techniques rapidly become more difficult to apply as the number of electrons studied increases, we discuss this approach only briefly, referring the interested reader to a recent review by Drake (1996).

Over the years, increasingly accurate solutions to the spectrum of helium have been obtained in roughly three stages. As just mentioned, the first accurate variational calculations were made by Hylleraas (1928, 1929) shortly after the introduction of the Schrödinger equation. After the introduction of computers, Kinoshita (1957) and later Accad *et al.* (1971) achieved much higher accuracy. Most recently, Drake (1996) and Morgan (1989) have achieved 16-digit and higher accuracy, the former by introducing two exponential scales and the latter by including certain logarithmic terms in the variational wave function we now describe.

The basic form of this wave function is

$$\Psi(\vec{r}_1,\vec{r}_2)=\sum_{i,j,k}a_{ijk}r_1^i r_2^j r_{12}^k e^{-\alpha r_1-\beta r_2}, \tag{51}$$

where exchange terms are implicit and we deal with S states. The angle dependence is contained in the $r_{12}=|\vec{r}_1-\vec{r}_2|$ terms. We note the similarity to the discussion of finite basis sets above. The sums are made finite by restricting the sum of i, j, and k to be less than or equal to Ω. A clear pattern of convergence is seen by increasing the maximum value of Ω. In the original calculations a very small number was used, but accuracies better than Hartree-Fock still resulted. The second stage of calculations used up to several hundred basis functions and achieved under 1 ppm accuracy, which is the level of QED radiative corrections. The most recent calculations achieve even higher accuracy by using the different forms mentioned above: Morgan includes another factor of the form $[\ln(r_1+r_2)]^l$, and Drake doubles the basis set by including another set of exponential parameters (α,β). While the accuracies achieved are well under experimental precision, this apparent "overkill" is actually necessary for the calculation of operator matrix elements. Because the approach is completely nonrelativistic, relativistic effects must be treated as perturbations, such as the relativistic mass increase operator $p^4/8m^3$. However, it is generally true that a method that

gives an accuracy of ϵ^2 for energies gives matrix elements accurate to order ϵ. Thus the very-high-accuracy methods of Drake and Morgan are required. Once the essentially exact nonrelativistic energies are combined with relativistic effects, comparison with experiment shows the presence of QED effects, just as in the sodiumlike platinum example. Here, of course, the effects are much smaller, entering at the ppm level rather than the percent level, and their evaluation requires a different form of QED, the Bethe-Salpeter equation.

Before we turn to a discussion of the all-orders methods and the Bethe-Salpeter equation, we mention recent progress in applying variational techniques to lithium (King, 1989; McKenzie and Drake, 1991; Yan and Drake, 1995). While considerably more computation is involved than in the case of helium, these calculations have been able to reach the nano-Hartree level. However, the difficulty of this kind of calculation grows extremely rapidly with the number of electrons, and other techniques must be used for atoms with large numbers of electrons.

A. All-orders methods and the Bethe-Salpeter equation for helium

A low-order MBPT calculation of helium energy levels, while sufficiently accurate for high Z, is inadequate for neutral helium, and some method for including all orders is required. In this section we make contact between a Green's function approach to atomic physics, the Bethe-Salpeter equation, and the first of the *all-orders* equations we shall discuss in this review. While the approaches seem quite different, with the former dealing with the position of poles in the electron-electron four-point function and the latter dealing directly with the Schrödinger equation, the end equations will be shown to be identical. We note that heliumlike ions have also been treated with the so-called ''unified method'' (Drake, 1988), with multiconfiguration Dirac-Fock (MCDF) methods (Hata and Grant, 1983, 1984; Indelicato *et al.*, 1988, 1987), and with Green's-functions methods (Shabaev, 1993).

In the following we concentrate on a relativistic calculation of the ground-state energy of helium, keeping only the effects of the Coulomb interaction. In this case the energy is known to be (Blundell *et al.*, 1989) $-2.903\,86$ a.u. Many-body perturbation theory through second order, starting from the Coulomb potential and the Hartree-Fock potential, gives results of $-2.907\,67$ a.u. and $-2.899\,05$ a.u., respectively. These differ from each other and the exact result at the level of a tenth of a percent, and it is clearly desirable to achieve higher accuracy. This can be done in two ways. The first is going to higher order in perturbation theory. The nonrelativistic (relativistic corrections are negligible) third-order MBPT results are (Musher and Shulman, 1968) 0.00434 a.u. for the $1/Z$ expansion case and -0.00377 a.u. for the HF case, which brings the results to within several hundredths of a percent of one another and the exact result. Rather than continue in this direction by going to fourth-order perturbation theory, we instead introduce a method that evaluates all orders of perturbation theory at once. This can be done by expressing the exact wave function in terms of products of the creation operator $a_i^\dagger$, which is an operator that creates an electron in one of the states i included in the basis set. Thus a general state of helium would be expressed as

$$\Psi=\sum_{ij}\rho_{ij}a_i^\dagger a_j^\dagger|0\rangle, \tag{52}$$

where we have for simplicity suppressed factors that create eigenstates of angular momentum. Knowledge of all the quantities ρ_{ij} then provides an exact description of the state, provided that a sufficiently large basis set is used. There are two ways to do this. One is an iterative procedure (Plante *et al.*, 1994). In this the above form for the wave function is used in the Schrödinger equation $(H_0+V)\Psi=E\Psi$ to obtain an equation for the coefficients ρ_{ij} of the form

$$(\epsilon_i+\epsilon_j)\rho_{ij}+\frac{1}{2}\sum_{kl}\tilde{g}_{ijkl}\rho_{kl}=E\rho_{ij}. \tag{53}$$

For the ground state, for example, one starts the iteration procedure by setting $E=2\epsilon_{1s}$, $\rho_{1s1s}=1$, and all other ρ's equal to zero. Then the above equation allows the generation of nonzero values for the other ρ's, and a convergent iterative scheme results. This procedure effectively sums up all orders of perturbation theory and gives results that agree with the known result for ground-state helium to about six digits. The other method is the configuration interaction method, in which the matrix equation is directly solved: an example of a very-large-scale relativistic configuration interaction calculation is the work of Chen and Cheng (1996). The main source of error in both methods is the fact that the partial-wave expansion, as described in the case of the second-order energy, cannot be directly summed to infinity. The relative slowness of convergence of the partial-wave expansion is connected to the existence of cusps in the wave function, which arise from the factor $r_<^l/r_>^{l+1}$ in the definition of the radial integral. An interesting recent development has been the demonstration by Goldman (1994, 1995, 1997) and Goldmann and Glickman (1997) that greatly increased convergence can be obtained by including $r_<$ and $r_>$ in the behavior of the wave function.

B. Relation to Green's-function methods

In this section we describe how the above reformulation of many-body perturbation theory can be related to a Green's-function approach to helium. In fact, the most accurate treatment of helium that incorporates QED is based on the Bethe-Salpeter equation, which in turn is based on a treatment of the four-point function (Araki, 1957; Sucher, 1957; Douglas and Kroll, 1974). We first introduce the electron propagator in the external field of the nucleus,

$$S(x,y)=\int \frac{dp_0}{2\pi}\, e^{-ip_0(x_0-y_0)}S(\vec{x},\vec{y};p_0), \tag{54}$$

where

$$S(\vec{x},\vec{y};p_0)=\sum_n \frac{\psi_n(\vec{x})\overline{\psi}_n(\vec{y})}{p_0-\epsilon_n(1-i\delta)} \tag{55}$$

satisfies the equation

$$\left[p_0\gamma_0+i\vec{\gamma}\cdot\vec{\nabla}_x+\frac{Z\alpha}{|\vec{x}|}\gamma_0-m\right]S(\vec{x},\vec{y};p_0)=\delta^3(\vec{x}-\vec{y}). \tag{56}$$

It is convenient to work with the Fourier transform of the above,

$$S(\vec{p},\vec{p}\,';p_0)=\sum_n \frac{\psi_n(\vec{p})\overline{\psi}_n(\vec{p}\,')}{p_0-\epsilon_n(1-i\delta)}. \tag{57}$$

The propagator for two electrons with total energy E interacting with the external field but not one another is then

$$S(E,k_0,\vec{k}_1,\vec{k}_2;\vec{k}_3,\vec{k}_4) =\sum_{mn} \frac{\psi_m(\vec{k}_1)\overline{\psi}_m(\vec{k}_3)}{E/2+k_0-\epsilon_m(1-i\delta)} \frac{\psi_n(\vec{k}_2)\overline{\psi}_n(\vec{k}_4)}{E/2-k_0-\epsilon_n(1-i\delta)}. \tag{58}$$

This propagator then enters the equation for the interacting two-electron propagator, or four-point function,

$$\begin{aligned}G(E;k_0,k_0';\vec{k}_1,\vec{k}_2;\vec{k}_3,\vec{k}_4)&=2\pi S(E;k_0;\vec{k}_1,\vec{k}_2;\vec{k}_3,\vec{k}_4)\,\delta(k_0-k_0')\\&\quad -i\int\frac{dp_0}{2\pi}\int d^3k_5d^3k_6d^3k_7d^3k_8 S(E;k_0;\vec{k}_1,\vec{k}_2;\vec{k}_5,\vec{k}_6)\\&\quad\times K(E;k_0,p_0,\vec{k}_5,\vec{k}_6;\vec{k}_7,\vec{k}_8)G(E;p_0,k_0';\vec{k}_7,\vec{k}_8;\vec{k}_3,\vec{k}_4),\end{aligned} \tag{59}$$

where K is the irreducible two-body kernel that is dominated by one-Coulomb photon exchange,

$$K_C(E;k_0,p_0,\vec{k}_5,\vec{k}_6;\vec{k}_7,\vec{k}_8) =-\frac{\alpha}{2\pi^2}\frac{\delta(\vec{k}_8+\vec{k}_7-\vec{k}_5-\vec{k}_6)}{|\vec{k}_5-\vec{k}_7|^2}, \tag{60}$$

and we have suppressed exchange terms. At this point we note that G has poles at the bound-state energies of helium, and near a pole of energy E_0 must behave as

$$G\to\frac{\psi_n(\vec{k}_1,\vec{k}_2;k_0)\overline{\psi}_n(\vec{k}_3,\vec{k}_4;k_0')}{E-E_0}. \tag{61}$$

While the noninteracting propagator has poles at bound-state energies that are the sums of the individual hydrogenic bound-state energies, these are at different positions from the full energy, so the inhomogeneous term drops out if we multiply by $E-E_0$ and take the limit $E\to E_0$. This results in the Bethe-Salpeter equation for helium,

$$\begin{aligned}\psi_0(k_0;\vec{k}_1,\vec{k}_2)=-i\int\frac{dp_0}{2\pi}\int d^3k_5d^3k_6d^3k_7d^3k_8&\\\times S(E_0;k_0;\vec{k}_1,\vec{k}_2;\vec{k}_5,\vec{k}_6)&\\\times K(E_0;k_0,p_0,\vec{k}_5,\vec{k}_6;\vec{k}_7,\vec{k}_8)&\\\times\psi_0(p_0;\vec{k}_7,\vec{k}_8),&\end{aligned} \tag{62}$$

which is still exact in this form.

If we replace the kernel with its dominant part K_C, we can exploit the fact that there is no dependence on k_0 or p_0 in that kernel (a well-defined perturbation theory allows inclusion of the full kernel). This is done by integrating the equation over k_0 and defining a new wave function

$$\phi_0(\vec{k}_1,\vec{k}_2)=\int dk_0\psi_0(k_0,\vec{k}_1,\vec{k}_2). \tag{63}$$

The integral over k_0 of $S(E_0;k_0;\vec{k}_1,\vec{k}_2;\vec{k}_3,\vec{k}_4)$ is exactly of the form given in Eq. (48). As in the treatment discussed there, we make the further approximation of keeping only the positive-energy states, treating the negative-energy-state contribution as a perturbation. We then have

$$\begin{aligned}\phi_0(\vec{k}_1,\vec{k}_2)=\frac{\alpha}{2\pi^2}\sum_{m_+n_+}\int d^3k_3d^3k_4d^3k_5&\\\times\frac{\psi_m(\vec{k}_1)\overline{\psi}_m(\vec{k}_3)\psi_n(\vec{k}_2)\overline{\psi}_n(\vec{k}_4)}{E_n-\epsilon_m-\epsilon_n}&\\\times\frac{1}{|\vec{k}_5-\vec{k}_3|^2}\phi_0(\vec{k}_5,\vec{k}_3+\vec{k}_4-\vec{k}_5).&\end{aligned} \tag{64}$$

If we operate on this equation with the operator $E_0-H(\vec{k}_1)-H(\vec{k}_2)$ and further define a projection operator

$$\Lambda_{++}(\vec{k}_1,\vec{k}_2;\vec{k}_3,\vec{k}_4) =\sum_{m_+n_+}\psi_m(\vec{k}_1)\overline{\psi}_m(\vec{k}_3)\psi_n(\vec{k}_2)\overline{\psi}_n(\vec{k}_4), \tag{65}$$

we find

TABLE IV. MBPT results for lithium energies: units a.u.

	$2s_{1/2}$	$2p_{1/2}$	$2p_{3/2}$	$3s_{1/2}$
$E(0)$	−0.19632	−0.12864	−0.12864	−0.07380
$E(2)$	−0.00165	−0.00137	−0.00137	−0.00035
Sum	−0.19797	−0.13001	−0.13001	−0.07415
Expt.	−0.19814	−0.13024	−0.13024	−0.07418

$$[E_n - H(\vec{k}_1) - H(\vec{k}_2)]\phi_0(\vec{k}_1,\vec{k}_2) = -\frac{\alpha}{2\pi^2}\int d^3k_3 d^3k_4 d^3k_5 \Lambda_{++}(\vec{k}_1,\vec{k}_2;\vec{k}_3,\vec{k}_4) \times \frac{1}{|\vec{k}_3-\vec{k}_5|^2}\phi_0(\vec{k}_5,\vec{k}_3+\vec{k}_4-\vec{k}_5). \quad (66)$$

The final step is to insert an extra positive-energy projector in between the Coulomb interaction and the wave function, which induces another small perturbation term involving $(1-\Lambda_{++})$, after which we finally end up with the so-called Coulomb-ladder equation (Douglas and Kroll, 1974),

$$[E_n - H(\vec{k}_1) - H(\vec{k}_2)]\phi_0(\vec{k}_1,\vec{k}_2) = \int d^3k_3 d^3k_4 d^3k_5 d^3k_6 d^3k_7 \Lambda_{++}(\vec{k}_1,\vec{k}_2;\vec{k}_3,\vec{k}_4) \times \frac{\alpha}{|\vec{k}_5-\vec{k}_3|^2}\Lambda_{++}(\vec{k}_5,\vec{k}_3+\vec{k}_4-\vec{k}_5;\vec{k}_6,\vec{k}_7) \times \phi_0(\vec{k}_6,\vec{k}_7). \quad (67)$$

The projection operators in the above equation serve to eliminate any negative-energy-state components of the wave function. At this point the above equation can be recognized as precisely the ''all-orders'' equation we introduced to sum all orders of MBPT. Specifically, we first represent the wave function in a manner analogous to Eq. (52),

$$\phi_0(\vec{k}_1,\vec{k}_2) = \sum_{ij} \rho_{ij}\psi_i(\vec{k}_1)\psi_j(\vec{k}_2), \quad (68)$$

with the understanding that the sum includes only positive-energy states. The two projection operators involve a sum over four positive-energy states, and there remains an integral that can be recognized as the Fourier transform of g_{ijkl}. Finally, multiplying the left- and right-hand sides of the equation by $\overline{\psi_i}(\vec{k}_1)$ and $\overline{\psi_j}(\vec{k}_2)$ followed by integrating over $\vec{k}_1$ and $\vec{k}_2$ gives an equation for the ρ_{ij} coefficients identical, except for the exchange term we have suppressed, to that described in the previous section.

After that equation is solved, of course, the small perturbations associated with the two steps involving projection operators above must be included, as well as the non-one-Coulomb exchange kernels. This perturbation theory has been carried out to the order of α^4 Rydbergs for the splitting of 2P states in neutral helium (Douglas and Kroll, 1974), and present interest is in calculation of the order of α^5 Rydberg contributions (Zhang and Drake, 1996).

It should be stressed that this way of framing MBPT within QED is different from the S-matrix approach previously described: the wave function in the S matrix has only whatever correlation is built in by the choice of the potential, while ϕ_0 sums an infinite set of ladder diagrams. For highly charged ions, the rapid convergence of perturbation theory makes either approach valid, but the breakup of perturbation theory is quite different. The extension of the Green's-function approach to more complicated atoms is a fundamental problem in QED, but as stressed above, we first need to understand how well all-orders methods work for these atoms. We now introduce this problem by discussing the behavior of MBPT for the neutral alkalis.

V. NEUTRAL ALKALI ATOMS

A. Energy calculations through second order

We have illustrated in the QED section the behavior of many-body perturbation theory for highly charged ions. Treatment of low orders succeeded because of the $1/Z$ expansion, but for valence electrons of many-electron neutral atoms, even when Z is high, almost all nuclear charge is screened, and there is no reason to believe that MBPT in low orders will work as well for neutral atoms as for highly charged ions. We illustrate the situation for the application of MBPT through second order for the alkali-metal atoms in Tables IV–IX

TABLE V. MBPT results for sodium energies: units a.u.

	$3s_{1/2}$	$3p_{1/2}$	$3p_{3/2}$	$4s_{1/2}$
$E(0)$	−0.18203	−0.10945	−0.10942	−0.07016
$E(2)$	−0.00587	−0.00178	−0.00177	−0.00125
Sum	−0.18790	−0.11123	−0.11119	−0.07141
Expt.	−0.18886	−0.11160	−0.11152	−0.07158

TABLE VI. MBPT results for potassium energies: units a.u.

	$4s_{1/2}$	$4p_{1/2}$	$4p_{3/2}$	$5s_{1/2}$
$E(0)$	−0.14749	−0.09571	−0.09550	−0.06109
$E(2)$	−0.01245	−0.00462	−0.00455	−0.00286
Sum	−0.15994	−0.10033	−0.10005	−0.06395
Expt.	−0.15952	−0.10035	−0.10009	−0.06371

TABLE VII. MBPT results for rubidium energies: units a.u.

	$5s_{1/2}$	$5p_{1/2}$	$5p_{3/2}$	$6s_{1/2}$
$E(0)$	−0.13929	−0.09082	−0.08999	−0.05870
$E(2)$	−0.01501	−0.00544	−0.00519	−0.00346
Sum	−0.15430	−0.09626	−0.09518	−0.06216
Expt.	−0.15351	−0.09619	−0.09511	−0.06177

TABLE VIII. MBPT results for cesium energies: units a.u.

	$6s_{1/2}$	$6p_{1/2}$	$6p_{3/2}$	$7s_{1/2}$
$E(0)$	−0.12737	−0.08562	−0.08378	−0.05519
$E(2)$	−0.01774	−0.00691	−0.00618	−0.00420
Sum	−0.14511	−0.09253	−0.08996	−0.05939
Expt.	−0.14310	−0.09217	−0.08964	−0.05865

taken from Johnson *et al.* (1996). The calculations are complete in the sense that all core states are summed over and very complete basis sets were used to essentially eliminate basis-set truncation error, and finally the partial-wave expansion is extrapolated to infinity.

We have several comments concerning these results. The first is that the Hartree-Fock energies start off accurate to about one percent for lithium, but degenerate to worse than ten percent for the heavy alkalis. Inclusion of second-order MBPT then significantly improves agreement with experiment, from one-tenth-of-a-percent accuracy for lithium to one or two percent for francium. The very good agreement at potassium is fortuitous, arising from the fact that the second-order energy underestimates correlation for light alkalis and overestimates it for heavy alkalis, with potassium near the crossover point. This behavior seems promising for the application of low-order MBPT, but in fact when we calculate the next order we shall see that this is not the case. Before that, we review the situation for transition matrix elements.

B. Matrix elements

While the calculation of energies is a good test of many-body perturbation theory, one is often more interested in other properties of the atom, for example hyperfine constants and oscillator strengths. In particular, parity-nonconserving transitions are a kind of oscillator strength, but with one state of the "wrong" parity because of the weak interactions. The first two orders of MBPT for matrix elements in alkalis can be set up in a straightforward way. We deal with a general one-body operator

$$Z=\sum_{ij} z_{ij}a_i^\dagger a_j . \tag{69}$$

If we call the initial state v and the final state w, the lowest and first orders are given by

TABLE IX. MBPT results for francium energies: units a.u.

	$7s_{1/2}$	$7p_{1/2}$	$7p_{3/2}$	$8s_{1/2}$
$E(0)$	−0.13107	−0.08591	−0.08044	−0.05596
$E(2)$	−0.02164	−0.00840	−0.00612	−0.00478
Sum	−0.15271	−0.09431	−0.08656	−0.06074
Expt.	−0.14967	−0.09392	−0.08623	

TABLE X. E_1 transition amplitudes for light alkalis.

Atom	Lithium	Sodium	Potassium
Transition	$2p_{1/2}\rightarrow 2s_{1/2}$	$3p_{1/2}\rightarrow 3s_{1/2}$	$4p_{1/2}\rightarrow 4s_{1/2}$
$Z^{(1)}$	3.3644	3.6906	4.5546
$Z^{(2)}$	−0.0116	−0.0385	−0.1578
$Z^{(3)}_{\rm RPA}$	−0.0019	−0.0034	0.0132
$Z^{(4+)}_{\rm RPA}$	−0.0004	−0.0013	−0.0094
$Z^{(3)}_{\rm BO}$	−0.0239	−0.1021	−0.3129
$Z^{(3)}_{\rm SR}$	0.0007	0.0030	0.0173
$Z^{(3)}_{\rm Norm}$	−0.0013	−0.0050	−0.0235
Sum	3.3260	3.5433	4.0815
Experiment	3.317(4)	3.525(2)	4.102(5)

$$Z^{(1)}=z_{wv}+\delta_{wv}\sum_a z_{aa} \tag{70}$$

and

$$Z^{(2)}=\sum_{am}\frac{z_{am}\tilde{g}_{wmva}}{\epsilon_{av}-\epsilon_{mw}}+\sum_{am}\frac{\tilde{g}_{wavm}z_{ma}}{\epsilon_{aw}-\epsilon_{mv}}. \tag{71}$$

We have specialized to the Hartree-Fock potential. The next order is somewhat complex, and we divide it into $Z^{(3)}=Z^{(3)}_{\rm RPA}+Z^{(3)}_{\rm BO}+Z^{(3)}_{\rm SR}+Z^{(3)}_{\rm Norm}$. The first term is given by

$$Z^{(3)}_{\rm RPA}=\sum_{abmn}\left[\frac{\tilde{g}_{wnva}z_{bm}\tilde{g}_{amnb}}{(\epsilon_{mw}-\epsilon_{bv})(\epsilon_{nw}-\epsilon_{av})}+\text{c.c.}\right]+\sum_{abmn}\left[\frac{\tilde{g}_{mnab}z_{bm}\tilde{g}_{awvn}}{(\epsilon_{nv}-\epsilon_{aw})(\epsilon_{mw}-\epsilon_{bv})}+\text{c.c.}\right]. \tag{72}$$

The notation c.c. refers to complex-conjugate terms that are obtained graphically by reflection about a horizontal axis. $Z^{(2)}$ and $Z^{(3)}_{\rm RPA}$ are the first two terms in the well-known RPA series. This series can be summed to infinity, and this will be done in the tabulations below. A point of note is that the usual method of summing involves solving differential equations, which automatically include both negative- and positive-energy intermediate states. Thus small differences arise when the above formulas are used with the usual restriction of allowing only positive-energy intermediate states. This point is addressed in greater detail by Johnson *et al.* (1995).

The next term is referred to as a Brueckner-orbital correction. It is given by

$$Z^{(3)}_{\rm BO}=\sum_{abmi}\left[\frac{g_{abmv}z_{wi}\tilde{g}_{miba}}{(\epsilon_i-\epsilon_v)(\epsilon_{vm}-\epsilon_{ab})}+\text{c.c.}\right]+\sum_{abmi}\left[\frac{g_{aimn}z_{wi}\tilde{g}_{mnav}}{(\epsilon_i-\epsilon_v)(\epsilon_{nm}-\epsilon_{av})}+\text{c.c.}\right]. \tag{73}$$

This term is closely related to the second-order energy and plays a particularly important role numerically, which is associated with the fact that the second-order energy is relatively large, particularly in the case of the heavier alkalis. The remaining parts of $Z^{(3)}$ are numeri-

TABLE XI. E_1 transition amplitudes for heavy alkalis.

Atom Transition	Rubidium $5p_{1/2}\rightarrow 5s_{1/2}$	Cesium $6p_{1/2}\rightarrow 6s_{1/2}$	Francium $7p_{1/2}\rightarrow 7s_{1/2}$
$Z^{(1)}$	4.8189	5.2777	5.1437
$Z^{(2)}$	−0.2237	−0.3344	−0.4136
$Z^{(3)}_{\mathrm{RPA}}$	0.0280	0.0760	0.1092
$Z^{(4+)}_{\mathrm{RPA}}$	−0.0173	−0.0446	−0.0652
$Z^{(3)}_{\mathrm{BO}}$	−0.4183	−0.5816	−0.6375
$Z^{(3)}_{\mathrm{SR}}$	0.0269	0.0445	0.0580
$Z^{(3)}_{\mathrm{Norm}}$	−0.0332	−0.0508	−0.0629
Sum	4.1813	4.3868	4.1317
Experiment	4.231(3)	4.499(6)	

cally less important, and we refer the interested reader to Johnson *et al.* (1996) for more details. Reduced matrix elements for a transition of multipolarity JM, defined through

$$Z_{wv}=(-1)^{j_w-\mu_w}\begin{pmatrix} J & j_v & j_w \\ M & \mu_v & -\mu_w \end{pmatrix}\langle w||Z||v\rangle, \qquad (74)$$

are tabulated for the light alkalis in Table X and for the heavier alkalis in Table XI.

The most important thing to note about these results is that both the RPA and Brueckner-orbital contributions play important roles in bringing theory into relatively good agreement with experiment: particularly in cesium, a 17% disagreement is brought down to under 3% primarily because of the two contributions, which are at roughly the same level. Another feature of note is that high orders of the random-phase approximation contribute at the percent level for the heavy alkalis, which is an indication that all-orders methods will be necessary to reach precisions lower than 1%. As mentioned above, the SR (structural radiation) and Norm (normalization) terms are numerically less important. Again, as with energies, MBPT appears to be working at the tenth-of-a-percent level for light alkalis and the one percent level for heavy alkalis. However, to reach the tenth-of-a-percent level for the latter case, higher orders of MBPT must clearly be investigated, and we now turn to that topic.

C. Third-order many-body perturbation theory

It is possible, using the basis-set techniques described above, to carry out a complete calculation of all diagrams contributing to the third-order energy for alkali-like atoms and ions. While for the highly charged ion case these terms will be very small, they will be much more important for neutral atoms. The fact that each

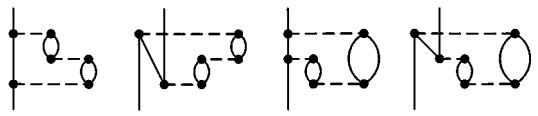

FIG. 4. Representative third-order Goldstone diagrams.

TABLE XII. Breakdown of third-order contributions as percentage of $6s_{1/2}$ Hartree-Fock energy of cesium.

Diagram	Percentage	Diagram	Percentage
A	3.2	G	0.3
B	−0.2	H	−0.2
C	−3.1	I	38.7
D	−0.3	J	−38.6
E	−3.3	K	1.4
F	0.1	L	−2.2

graph can be accurately evaluated will play an important role when we treat such systems with all-order methods. If an all-orders method, no matter how apparently elegant, does not include a third-order diagram that can be shown to be numerically significant, the method must be modified to include it.

There are 84 terms contributing to the third-order $E_v^{(3)}$ (we suppress the third-order core energy for the usual reasons). They can be written more compactly by including direct and exchange contributions together with the previously introduced notation $\tilde{g}_{ijkl}=g_{ijkl}-g_{ijlk}$. Then an algebraic or graphical derivation leads to 12 terms,

$$E_A^{(3)}=\sum_{abmnr}\frac{\tilde{g}_{vbmr}\tilde{g}_{mnva}\tilde{g}_{mnva}}{(\epsilon_{av}-\epsilon_{mn})(\epsilon_{bv}-\epsilon_{rm})},$$

$$E_B^{(3)}=-\sum_{abcmn}\frac{\tilde{g}_{canv}\tilde{g}_{nbcm}\tilde{g}_{mvba}}{(\epsilon_{ac}-\epsilon_{nv})(\epsilon_{ab}-\epsilon_{vm})},$$

$$E_C^{(3)}=\sum_{abmnr}\frac{\tilde{g}_{avmn}\tilde{g}_{nbvr}\tilde{g}_{mrab}}{(\epsilon_{av}-\epsilon_{mn})(\epsilon_{ab}-\epsilon_{rm})}+\text{c.c.},$$

$$E_D^{(3)}=-\sum_{abcmn}\frac{\tilde{g}_{abnv}\tilde{g}_{vcbm}\tilde{g}_{nmac}}{(\epsilon_{ab}-\epsilon_{vn})(\epsilon_{ac}-\epsilon_{mn})}+\text{c.c.},$$

$$E_E^{(3)}=\sum_{amnrs}\frac{\tilde{g}_{avsr}g_{rsnm}g_{mnav}}{(\epsilon_{av}-\epsilon_{mn})(\epsilon_{av}-\epsilon_{rs})},$$

$$E_F^{(3)}=-\sum_{abcdm}\frac{\tilde{g}_{cdmv}g_{abcd}g_{mnab}}{(\epsilon_{ab}-\epsilon_{vm})(\epsilon_{cd}-\epsilon_{vm})},$$

$$E_G^{(3)}=-\sum_{abmnr}\frac{g_{abrv}g_{rvmn}\tilde{g}_{mnab}}{(\epsilon_{ab}-\epsilon_{vr})(\epsilon_{ab}-\epsilon_{mn})}+\text{c.c.},$$

$$E_H^{(3)}=\sum_{abcmn}\frac{g_{avmn}g_{bcva}\tilde{g}_{mncb}}{(\epsilon_{av}-\epsilon_{mn})(\epsilon_{bc}-\epsilon_{mn})}+\text{c.c.},$$

$$E_I^{(3)}=-\sum_{abcmn}\frac{\tilde{g}_{acmn}\tilde{g}_{vbvc}g_{mnab}}{(\epsilon_{ac}-\epsilon_{mn})(\epsilon_{ab}-\epsilon_{mn})},$$

$$E_J^{(3)}=\sum_{abmnr}\frac{\tilde{g}_{abrn}\tilde{g}_{vrvm}g_{mnab}}{(\epsilon_{ab}-\epsilon_{rn})(\epsilon_{ab}-\epsilon_{mn})},$$

$$E_K^{(3)}=-\sum_{abcmn}\frac{\tilde{g}_{vavm}g_{cban}\tilde{g}_{mncb}}{(\epsilon_{a}-\epsilon_{m})(\epsilon_{bc}-\epsilon_{mn})}+\text{c.c.},$$

$$E_L^{(3)}=\sum_{abmnr}\frac{\tilde{g}_{vavm}g_{bmnr}\tilde{g}_{rnab}}{(\epsilon_{a}-\epsilon_{m})(\epsilon_{ab}-\epsilon_{nr})}+\text{c.c.} \qquad (75)$$

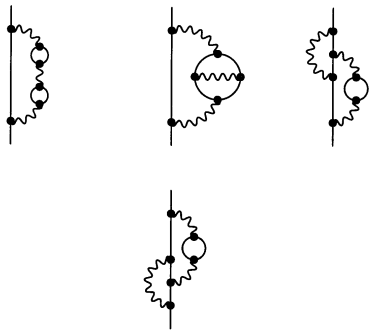

FIG. 5. Feynman diagrams contributing to the third-order energy.

Examples of the associated Brueckner-Goldstone diagrams are shown in Fig. 4. The most difficult computationally is $E_E^{(3)}$ because of the fourfold summation over excited states. However, all terms can be evaluated in a matter of hours on modern workstations, though the partial-wave expansion of the term just mentioned cannot be treated as thoroughly as the others. We collect the results of a third-order calculation (Blundell *et al.*, 1990) in Table XII.

One of the most striking features of the third-order energy is the very large but canceling contributions from diagrams I and J. These come from factors with large overlap of the wave function, but general arguments can be made (Sushkov, 1986) that explain the almost complete cancellation. Of the remaining diagrams, A, C, E, and K are the most important. However, to reach a precision of 0.1%, each diagram must be included. The net result, unfortunately, takes the energy from 1.4% too large to 2.5% too small in magnitude. Thus straightforward perturbation theory is not converging in a uniform manner, and higher orders must be treated in some fashion.

It is also possible to reorganize the third order calculation in terms of Feynman diagrams (Dzuba *et al.*, 1989). The Novosibirsk group evaluate the four Feynman diagrams shown in Fig. 5. These can be shown to account for the largest of the third-order diagrams; however, diagrams not included amount to about two percent of the valence energy. Thus the agreement between theory and experiment found by that group presumably relies upon cancellation of uncalculated terms.

D. All-orders methods

One possibility that one can consider at this point is the direct investigation of all fourth-order many-body perturbation diagrams affecting the energy. However, several hundred diagrams would have to be considered, and we are not aware that they have even been tabulated for the open-shell case, although they have for the closed-shell (Wilson, 1985). It is possible explicitly to evaluate individual fourth-order diagrams that might be expected to be important. This was done by Blundell *et al.* (1990), who included the diagrams of Fig. 6. While

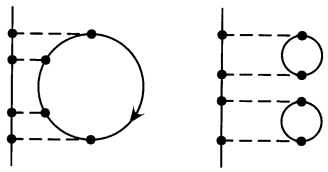

FIG. 6. Numerically important fourth-order Goldstone diagrams.

they had in fact the effect of bringing the energy into agreement with experiment, this is not a satisfactory procedure, and some method of treating all, or at least the most important, sets of fourth-order diagrams, is needed. Such a method is afforded by the use of the all-orders methods we have already discussed in connection with helium. All-orders methods not only generate infinite classes of diagrams, but can also generate many different diagrams in a given order in a compact manner. We now describe a particular all-orders method that was used for high-accuracy calculation of parity nonconservation in cesium (Blundell *et al.*, 1992).

As in the case with helium, we consider the structure of the wave function written in second-quantized form. For an alkali, the first-order correction to the ground-state wave function, $\Psi_0 \equiv a_v^\dagger |0_C\rangle$, is

$$|1_C\rangle = \left(\sum_{amn} \frac{g_{nmva}}{\epsilon_{mn} - \epsilon_{av}} a_m^\dagger a_n^\dagger a_a a_v + \frac{1}{2} \sum_{abmn} \frac{g_{mnba}}{\epsilon_{mn} - \epsilon_{ab}} a_m^\dagger a_n^\dagger a_b a_a \right) \Psi_0 , \tag{76}$$

where we have assumed that the potential is Hartree-Fock. When $|2_C\rangle$ is calculated, similar structures arise (Blundell *et al.*, 1987), such as

$$|2_C\rangle_a = \sum_{amnrs} \frac{g_{nmrs} g_{rsav}}{(\epsilon_{mn} - \epsilon_{av})(\epsilon_{rs} - \epsilon_{av})} a_m^\dagger a_n^\dagger a_a a_v \Psi_0 . \tag{77}$$

We refer to such terms as *double excitations* because two electrons (one core electron a and the valence electron v) have been destroyed and replaced with excited states. Such terms enter in each order of perturbation theory, and it rapidly becomes impractical to evaluate them explicitly in higher orders. However, it is possible to do this in another way, by treating the coefficient of $a_m^\dagger a_n^\dagger a_a a_v \Phi_0$ as an unknown coefficient ρ_{mnva}. This quantity is a generalization of the ρ_{ij} coefficients introduced in the case of helium. We note the difference that in the case of helium the vacuum was the true vacuum, while here we work relative to a filled core plus valence state. Thus there is a set of coefficients that can be ordered with respect to how many electrons of the atom are destroyed and replaced with excited states, which we call singles, doubles, triples, etc. Explicitly, we assume the following form for the wave function:

$$\Psi = N_v \Bigg(1 + \sum_{am} \rho_{ma} a_m^\dagger a_a + \sum_m{}' \rho_{mv} a_m^\dagger a_v + \frac{1}{2} \sum_{abmn} \rho_{mnab} a_m^\dagger a_n^\dagger a_b a_a + \sum_{amn} \rho_{mnva} a_m^\dagger a_n^\dagger a_a a_v + \sum_{abcmnr} \rho_{mnrabc} a_m^\dagger a_n^\dagger a_r^\dagger a_c a_b a_a + \sum_{abmnr} \rho_{mnrvab} a_m^\dagger a_n^\dagger a_r^\dagger a_b a_a a_v \Bigg) \Psi_0 , \tag{78}$$

where N_v is a normalization factor. The second and third terms describe single excitations, the third and fourth double excitations, and the last two triple excitations. Substituting this form for the wave function into the Schrödinger equation, one obtains a set of coupled equations for the expansion coefficients. If we make the approximation of neglecting the effect of the triple excitations on the right-hand side of the equation for triples, the following set of equations results:

$$(\epsilon_m - \epsilon_a - \delta E_v)\rho_{ma} = \sum_{bn} \rho_{nb} \tilde{g}_{bman} + \sum_{bcn} \tilde{g}_{bcan} \rho_{nmcb} + \sum_{bnr} \tilde{g}_{bmnr} \rho_{rnba} , \tag{79}$$

$$(\epsilon_m - \epsilon_v - \delta E_v)\rho_{mv} = \sum_{an} \rho_{na} \tilde{g}_{amvn} + \sum_{abn} \tilde{g}_{abnv} \rho_{nmab} + \sum_{anr} \tilde{g}_{amnr} \rho_{nrva} + \sum_{abnr} \tilde{g}_{abnr} (\rho_{rnmvab} - \rho_{rmnvab} + \rho_{mrnvab}), \tag{80}$$

$$\begin{aligned}(\epsilon_{mn} - \epsilon_{av} - \delta E_v)\rho_{mnva} = & -g_{mnva} + \sum_{rs} g_{mnrs} \rho_{srva} + \sum_{bc} g_{bcva} \rho_{nmbc} + \sum_r \rho_{ra} g_{mnrv} + \sum_r \rho_{rv} g_{nmra} + \sum_b \rho_{nb} g_{bmav} \\ & + \sum_b \rho_{mb} g_{bnva} + \sum_{br} \tilde{g}_{bmrv} \tilde{\rho}_{rnab} + \sum_{br} \tilde{g}_{bnra} \tilde{\rho}_{rmvb} + \sum_{brs} \tilde{g}_{bmrs} (\rho_{snrvab} + \rho_{rnsvab} - \rho_{nrsvab}) \\ & + \sum_{bcr} \tilde{g}_{cbra} (-\rho_{rnmvbc} + \rho_{nrmvbc} - \rho_{nmrvbc}),\end{aligned} \tag{81}$$

$$\begin{aligned}(\epsilon_{mn} - \epsilon_{ab} - \delta E_v)\rho_{mnab} = & -g_{mnab} + \sum_{rs} g_{mnsr} \rho_{rsab} - \sum_{cd} g_{cdab} \rho_{mncd} + \sum_c (\rho_{nc} g_{cmba} + \rho_{mc} g_{cnab}) + \sum_r (\rho_{rb} g_{mnra} \\ & + \rho_{ra} g_{nmrb}) + \sum_{cr} (\tilde{g}_{cmbr} \tilde{\rho}_{rnac} + \tilde{g}_{cnar} \tilde{\rho}_{rmbc}),\end{aligned} \tag{82}$$

$$\begin{aligned}(\epsilon_{mnr} - \epsilon_{abv} - \delta E_v)\rho_{mnrvab} = & -\rho_{rb} g_{mnva} + \frac{1}{2} \rho_{rv} g_{mnba} + \sum_c \tilde{g}_{crbv} \rho_{mnac} + \sum_s g_{mnsv} \rho_{srab} - \sum_c g_{cmba} \rho_{nrvc} \\ & + \sum_s g_{mnsa} \tilde{\rho}_{rsvb} + \cdots ,\end{aligned} \tag{83}$$

where

$$\delta E_v = \sum_{amn} \tilde{g}_{vamn} \rho_{mnva} + \sum_{abm} \tilde{g}_{abvm} \rho_{mvab} + \sum_{am} \tilde{g}_{vavm} \rho_{ma} + \sum_{abmn} \tilde{g}_{abmn} (\rho_{vmnvab} + \rho_{nvmvab} + \rho_{mnvvab}). \tag{84}$$

While this approach is formally quite similar to configuration interaction methods, an important difference is that unlinked terms involving the shift in the core energy δE_c have dropped out of the above equations: in a configuration interaction approach one would, for example, encounter factors such as $(\epsilon_m - \epsilon_a - \delta E_v - \delta E_c)$ rather than $(\epsilon_m - \epsilon_a - \delta E_v)$ multiplying ρ_{ma}.

We begin the discussion of these equations by neglecting the triple excitation terms. If one approximates the equation for ρ_{mnav} by dropping δE_v and keeps only the first term on the right-hand side, one sees that this reproduces the analogous term in $|1_C\rangle$. Further, by taking this form and adding it perturbatively to the second term, one can see the origin of $|2_C\rangle_a$. However, when one iterates the entire set of equations, an approximation to the wave function results that encompasses large parts of arbitrarily high-order contributions to the wave function. Convergence to six digits can be achieved with a sufficient number of iterations, though, because of the neglected triples, agreement with experiment at this level need not necessarily be expected. It is possible to trace the effect of this approximation on the third-order energy. While the second-order energy is entirely accounted for, 36 of the 84 third-order diagrams are left out. These can be added perturbatively, or they can also be obtained by including the triples coefficient in the equation for the singles coefficient ρ_{mv}. It is this procedure that is followed in the calculations of parity nonconservation in cesium reported by Blundell *et al.* (1992). As an example of the kind of accuracies that are reached with this method, we show in Table XIII a comparison of theory and experiment for a few energy levels

TABLE XIII. All-orders results for cesium energies: units a.u.

	$6s_{1/2}$	$6p_{1/2}$	$6p_{3/2}$	$7s_{1/2}$
$E(0)$	−0.12737	−0.08562	−0.08378	−0.05519
$E(2-\infty)$	−0.01521	−0.00636	−0.00572	−0.00326
Sum	−0.14257	−0.09198	−0.08951	−0.05845
Expt.	−0.14310	−0.09217	−0.08964	−0.05865

in cesium. It can be seen that agreement with experiment at the level of a few tenths of a percent has been reached. In Table XIV we also show the results of the Novosibirsk group (Dzuba *et al.*, 1989) and a singles-doubles coupled-cluster method based on Gaussian basis sets (Eliav *et al.*, 1994, for the same energy levels, which are even closer to experiment. While this is empirical evidence that the terms not included by the different calculations are relatively small, the next step is clearly to introduce methods that include more diagrams to ensure that the agreement with experiment is not because of fortuitous cancellations.

A first step in this direction is a more complete treatment of triples. While the entire third-order energy is accounted for by including the effect of triples on the singles coefficient, we have not included the effect of the triples on the equation for the doubles coefficient ρ_{mnav}, and this means certain fourth-order diagrams have been omitted. There is no problem in principle with carrying out this calculation, although computationally it is extremely intensive. We note in passing that the third-order energy actually contains only double-excitation-type denominators, and that singles-doubles methods can be devised that pick up the entire third-order energies, notably the Hermitian formalism of Lindgren (1991).

A more challenging numerical issue is iterating the equation for the triples coefficient itself: in the equation for the triples given above, we kept only those terms on the right-hand side that involved singles and doubles. Because of the large size of the basis set needed for accurate cesium calculations, direct storage of the triple excitation coefficients is difficult unless the size of the basis set is reduced to a point where basis-set truncation error becomes a problem. However, given advances in the memory and speed of computers, it is likely that these problems will be overcome, and then an almost complete set of fourth-order diagrams will be accounted for. It seems highly likely that at this point theoretical predictions reliable to the tenth-of-a-percent level for neutral alkalis will be forthcoming and that a proper treatment of field-theoretic effects will become necessary.

A last set of fourth-order diagrams is associated with the coupled-cluster method (Bishop and Kummel, 1987; Bartlett, 1991). The all-orders method we have presented is essentially a linearized version of that method. If we rewrite our representation of the wave function as

$$\Psi = N_v(1 + X_1 + X_2 + X_3 + \cdots)\Psi_0, \tag{85}$$

with X_1 a shorthand for single excitations, etc., we can write the coupled-cluster form as

$$\Psi = N_v e^{S_1 + S_2 + S_3 + \cdots}\Psi_0. \tag{86}$$

Here it is understood that the coefficients S are represented by connected diagrams, as opposed to the coefficients X, which are represented by both connected and disconnected graphs. Doing this automatically accounts for certain corrections to the wave function that would in the linearized method described here be categorized as quadruple excitations. Explicitly, the second-order correction to the wave function consists of singles, doubles, and triples, plus one extra term (Blundell *et al.*, 1987),

$$\Psi_4 = \frac{1}{4}\sum_{abcdmnrs} \frac{g_{mnab}g_{srcd}}{(\epsilon_{mn} - \epsilon_{ab})(\epsilon_{mnrs} - \epsilon_{abcd})} \times a_a a_b a_c a_d a_m^\dagger a_n^\dagger a_s^\dagger a_r^\dagger \Psi_0, \tag{87}$$

which upon symmetrization can be seen to be disconnected. However, this term can be identified as part of $\frac{1}{2}S_2^2\Psi_0$ and would be accounted for automatically in the full coupled-cluster method in second order, while it would not be picked up by the linearized method unless fourth-order terms were considered. We refer the interested reader to a calculation in this framework of energy levels of neutral sodium (Salomonson and Ynnerman, 1991).

VI. CONCLUSION

The first conclusion we should like to emphasize is that the atomic many-body problem is in principle extremely well understood, as it is directly based on QED. However, the Schrödinger equation is still difficult to solve, and the atomic many-body theorist faces the same numerical difficulties as many-body theorists in other fields. Two cases, however, stand out in which these difficulties can be circumvented; first, the spectroscopy of highly charged ions (where MBPT is rapidly convergent), and second, heliumlike ions and helium, where

TABLE XIV. Comparison of different calculations of cesium energies: units a.u.

	$6s_{1/2}$	$6p_{1/2}$	$6p_{3/2}$	$7s_{1/2}$
Eliav *et al.* (1994)	−0.14326	−0.09212	−0.08962	−0.05867
Dzuba *et al.* (1989)	−0.14325	−0.09214	−0.08961	−0.05889
Blundell *et al.* (1992)	−0.14257	−0.09198	−0.08951	−0.05845
Expt.	−0.14310	−0.09217	−0.08964	−0.05865

the structure problem can be treated exactly. In these cases, the interest shifts to the proper calculation of QED effects in many-electron systems. We have also treated the more difficult problem of neutral alkali atoms. In this case, law orders of MBPT can give results accurate at the percent level. It is only when the tenth-of-one-percent level is attempted that the full complexity of the many-body problem enters. While we have chosen to attack the problem with an all-orders approach based on including increasing numbers of excitations of core and valence electrons as the best method for reaching this level, many other many-body techniques have been developed by the community over the years, and it is quite possible that another method could prove more successful: one aim of this review is to stimulate the interest of many-body theorists in other fields who use different techniques, which may well be able to achieve higher accuracy. Given the great increase in computer power over the past few years and new developments in many-body theory, it is likely that the situation described in this review for few-electron atoms and highly charged ions, in which the Schrödinger equation can be solved to such precision that relativistic and QED effects have to be understood, will be repeated for more and more of the periodic table over the coming years.

ACKNOWLEDGMENTS

This work was supported in part by NSF grant PHY95-13179. Much of the research described was carried out in collaboration with Steven Blundell and Walter Johnson. I thank K.T. Cheng and S. Libby for useful comments and Steven Blundell for a careful reading of the manuscript.

REFERENCES

Accad, Y., C. L. Pekeris, and B. Schiff, 1971, Phys. Rev. A **4**, 516.
Araki, H., 1957, Prog. Theor. Phys. **17**, 619.
Barnett, R. N., E. M. Johnson, and W. A. Lester, 1995, Phys. Rev. A **51**, 2049.
Bartlett, R. J., 1991, Theor. Chim. Acta. **80**, 71.
Bishop, R., and H. Kummel, 1987, Phys. Today **40**, 42 (March).
Blundell, S. A., D. S. Guo, W. R. Johnson, and J. Sapirstein, 1987, At. Data Nucl. Data Tables **37**, 103.
Blundell, S. A., W. R. Johnson, Z. W. Liu, and J. Sapirstein, 1989, Phys. Rev. A **39**, 3768.
Blundell, S. A., W. R. Johnson, and J. Sapirstein, 1990, Phys. Rev. A **42**, 3751.
Blundell, S. A., W. R. Johnson, and J. Sapirstein, 1992, Phys. Rev. D **45**, 1602.
Blundell, S. A., and N. Snyderman, 1991, Phys. Rev. A **44**, R1427.
Bottcher, C., and M. R. Strayer, 1987, Ann. Phys. (N.Y.) **175**, 64.
Brandow, B. H., 1967, Rev. Mod. Phys. **39**, 771.
Brown, G. E., and D. G. Ravenhall, 1951, Proc. R. Soc. London, Ser. A **208**, 552.
Bunge, C. F., 1976, Phys. Rev. A **14**, 1965.
Carlsson, J., and L. Sturesson, 1989, Z. Phys. D **14**, 281.
Ceperley, D. M., and L. Mitas, 1996, in *Advances in Chemical Physics*, **93** (Wiley, New York), p. 1.
Chang, T. N., and X. Tang, 1991, Phys. Rev. A **44**, 232.
Chen, C.-C., 1993, J. Phys. B **26**, 599.
Chen, M., and K. T. Cheng, 1996, Phys. Rev. A **53**, 2206.
Cheng, K. T., W. R. Johnson, and J. Sapirstein, 1993, Phys. Rev. A **47**, 1817.
Chodos, A., R. L. Jaffe, K. Johnson, C. B. Thorn, and V. W. Weisskopf, 1974, Phys. Rev. D **9**, 3471.
Chung, Kwong T., X.-W. Zhu, and Z.-W. Wang, 1993, Phys. Rev. A **47**, 1740.
Cowan, R. D., 1981, *The Theory of Atomic Structure and Spectra* (University of California, Berkeley).
Cowan, T. E., C. L. Bennett, D. D. Dietrich, J. Bixler, C. J. Hailey, J. R. Henderson, D. A. Knapp, M. Levine, R. E. Marrs, and M. B. Schneider, 1991, Phys. Rev. Lett. **66**, 1150.
deBoor, C., 1978, *A Practical Guide to Splines* (Springer, New York).
Desclaux, J. P., 1975, Comput. Phys. Commun. **9**, 31.
Desclaux, J. P., 1977, Comput. Phys. Commun. **13**, 71.
Douglas, M., and N. Kroll, 1974, Ann. Phys. (N.Y.) **82**, 89.
Doyle, Holly Thomas, 1969, Adv. At. Mol. Phys. **5**, 337.
Drake, G. W. F., 1988, Can. J. Phys. **66**, 586.
Drake, G. W. F., 1996, in *Atomic, Molecular, and Optical Physics Handbook*, edited by Gordon W. F. Drake (AIP Press, Woodbury, NY), Chap. 11.
Dzuba, V. A., V. V. Flambaum, P. G. Silvestrov, and O. P. Sushkov, 1986, J. Phys. B **20**, 3297.
Dzuba, V. A., V. V. Flambaum, and O. Sushkov, 1989, Phys. Lett. A **140**, 493.
Dzuba, V. A., V. V. Flambaum, and O. P. Sushkov, 1995, Phys. Rev. A **51**, 3454.
Eliav, E., U. Kaldor, and Y. Ishikawa, 1994, Phys. Rev. A **50**, 1121.
Eliav, E., U. Kaldor, Y. Ishikawa, M. Seth, and P. Pykkö, 1996a, Phys. Rev. A **53**, 3926.
Eliav, E., U. Kaldor, Y. Ishikawa, and P. Pykkö, 1996b, Phys. Rev. Lett. **77**, 5350.
Fetter, A., and J. D. Walecka, 1971, *Quantum Theory of Many-Particle Systems* (McGraw-Hill, New York).
Froese Fischer, C., 1977, *The Hartree-Fock Method for Atoms: A Numerical Approach* (Wiley, New York).
Froese Fischer, C., 1986, Comput. Phys. Ref. **3**, 273.
Froese Fischer, C., W. Guo, and Z. Chen, 1992, Int. J. Quantum Chem. **42**, 849.
Fuhr, J. R., G. A. Martin, and W. L. Wiese, 1988, J. Phys. Chem. Ref. Data **17**, Suppl. 4.
Furry, W. H., 1951, Phys. Rev. **81**, 115.
Gaupp, A., P. Kuske, and H. J. Andrä, 1982, Phys. Rev. A **26**, 3351.
Gell-Mann, M., and F. Low, 1951, Phys. Rev. **84**, 350.
Goldman, S. P., 1994, Phys. Rev. Lett. **73**, 2547.
Goldman, S. P., 1995, Phys. Rev. A **52**, 3718.
Goldman, S. P., 1997, Phys. Rev. Lett. **78**, 2325.
Goldman, S. P., and T. Glickman, 1997, Phys. Rev. A **55**, 1772.
Goldstone, J., 1957, Proc. R. Soc. London, Ser. A **239**, 267.
Gorceix, O., and P. Indelicato, 1988, Phys. Rev. A **37**, 1087.
Grant, I. P., 1996, in *Atomic, Molecular, and Optical Physics Handbook*, edited by Gordon W. F. Drake (AIP Press, Woodbury, NY), Chap. 22.
Grant, I. P., B. J. McKenzie, P. H. Norrington, D. F. Mayers, and N. C. Pyper, 1980, Comput. Phys. Commun. **21**, 207.

Hansen, J. E., M. Bentley, H. W. van der Hart, M. Landtman, G. M. S. Lister, Y.-T. Shen, and N. Vaeck, 1993, Phys. Scr. **T47**, 7.
Hansen, J. E., and B. R. Judd, 1986, Comments At. Mol. Phys. **18**, 125.
Hata, J., and I. P. Grant, 1983, J. Phys. B **16**, 523.
Hata, J., and I. P. Grant, 1984, J. Phys. B **17**, 931.
Hylleraas, E. A., 1928, Z. Phys. **48**, 469.
Hylleraas, E. A., 1929, Z. Phys. **54**, 347.
Indelicato, P., 1988, Nucl. Instrum. Methods Phys. Res. B **31**, 14.
Indelicato, P., O. Gorceix, and J. P. Desclaux, 1987, J. Phys. B **20**, 651.
Indelicato, P., and E. Lindroth, 1992, Phys. Rev. A **46**, 2426.
Johnson, W. R., and K. T. Cheng, 1985, in *Atomic Inner-Shell Physics*, edited by Bernd Crasemann (Plenum, New York).
Johnson, W. R., D. S. Guo, M. Idrees, and J. Sapirstein, 1986, Phys. Rev. A **34**, 1043.
Johnson, W. R., Z. W. Liu, and J. Sapirstein, 1996, At. Data Nucl. Data Tables **64**, 279.
Johnson, W. R., D. R. Plante, and J. Sapirstein, 1995, in *Advances in Atomic, Molecular, and Optical Physics* **35** (Academic, New York), p. 255.
Johnson, W. R., and J. Sapirstein, 1986, Phys. Rev. Lett. **57**, 1126.
Kelly, H. P., 1964, Phys. Rev. **136**, 896.
King, F. W., 1989, Phys. Rev. A **40**, 1735.
Kinoshita, T., 1957, Phys. Rev. **105**, 1490.
Kragh, Helge, 1982, Centaurus **26**, 154.
Lindgren, I., 1990, J. Phys. B **23**, 1095.
Lindgren, I., 1991, J. Phys. B **24**, 1143.
Lindgren, I., and J. Morrison, 1986, *Atomic Many-Body Theory*, 2nd Ed. (Springer, New York).
Lindroth, E., 1988, Phys. Rev. A **37**, 316.
Lindroth, E. and P. Indelicato, 1994, Nucl. Instrum. Methods Phys. Res. B **87**, 22.
Lindroth, E., and A.-M. Martensson-Pendrill, 1989, Phys. Rev. A **39**, 3794.
Lindroth, E., H. Persson, S. Solomonson, and A.-M. Martensson-Pendrill, 1992, Phys. Rev. A **45**, 1493.
Lindroth, E., H. Persson, S. Solomonson, and A.-M. Martensson-Pendrill, 1995, Phys. Rev. A **51**, 297.
Liu, Z.-W., and H. P. Kelly, 1991, Phys. Rev. A **43**, 3305.
Mann, J. B., and W. R. Johnson, 1971, Phys. Rev. A **4**, 44.
Martensson-Pendrill, A. M., 1992, in *Methods in Computational Chemistry*, Vol. 5, edited by S. Wilson (Plenum, NY), p. 99.
McAlexander, W. L., E. R. I. Abraham, N. W. M. Ritchie, C. J. Williams, H. T. C. Stoof, and R. G. Hulet, 1995, Phys. Rev. A **51**, R871.
McKenzie, D. K., and G. W. F. Drake, 1991, Phys. Rev. A **44**, R6973.
McKenzie, B. J., I. P. Grant, and P. H. Norrington, 1980, Comput. Phys. Commun. **21**, 233.
McKoy, V., and N. W. Winter, 1968, J. Chem. Phys. **48**, 5514.
Mittelman, M. H., 1971, Phys. Rev. A **4**, 893.
Mittelman, M. H., 1981, Phys. Rev. A **24**, 1167.
Mittelman, M. H., 1989, Phys. Rev. A **39**, 1.
Mohr, P. J., 1992, Phys. Rev. A **46**, 4421.
Mohr, P. J., and Y. K. Kim, 1992, Phys. Rev. A **45**, 2727.
Morgan, J., 1989, in *Relativistic, Quantum Electrodynamic, and Weak Interaction Effects in Atoms*, Santa Barbara, California, 1989, AIP Conf. Proc. No. 189, edited by Walter Johnson, Peter Mohr, and Joseph Sucher (AIP, New York, 1989), p. 123.
Musher, J. I., and J. M. Shulman, 1968, Phys. Rev. **173**, 93.
Persson, H., I. Lindgren, S. Salomonson, and A. Ynnerman, 1993, Phys. Rev. A **47**, R4555.
Plante, D., W. R. Johnson, and J. Sapirstein, 1994, Phys. Rev. A **49**, 3519.
Salomonson, S., and P. Oster, 1989a, Phys. Rev. A **40**, 5548.
Salomonson, S., and P. Oster, 1989b, Phys. Rev. A **40**, 5559.
Salomonson, S., and P. Oster, 1990, Phys. Rev. A **41**, 4670.
Salomonson, S., and A. Ynnerman, 1991, Phys. Rev. A **43**, 88.
Sapirstein, J., 1989, in *Relativistic, Quantum Electrodynamic, and Weak Interaction Effects in Atoms*, Santa Barbara, California, 1989, AIP Conf. Proc. No. 189, edited by Walter Johnson, Peter Mohr, and Joseph Sucher (AIP, New York, 1989), p. 196.
Sapirstein, J., 1996, *Atomic, Molecular, and Optical Physics Handbook*, edited by Gordon W. F. Drake (AIP Press, Woodbury, NY), Chap. 29.
Sapirstein, J., and W. R. Johnson, 1996, J. Phys. B **29**, 5213.
Schiff, L., 1968, *Quantum Mechanics*, Third Edition (McGraw-Hill, New York), p. 263.
Schwartz, C., 1962, Phys. Rev. **126**, 1015.
Shabaev, V. M., 1993, J. Phys. B **26**, 4703.
Sinanoglu, O., and K. A. Brueckner, 1970, *Three Approaches to Electron Correlation in Atoms* (Yale University, New Haven).
Sobel'man, I. I., 1972, *Introduction to the Theory of Atomic Spectra* (Pergamon, Oxford).
Sucher, J., 1957, Phys. Rev. **107**, 1448.
Sucher, J., 1980, Phys. Rev. A **22**, 348.
Sucher, J., 1984, Int. J. Quantum Chem. **25**, 3.
Sushkov, O., 1986, private communication.
Volz, U., and H. Schmoranzer, 1996, Phys. Scr. **T65**, 48.
Wilson, S., 1985, Comput. Phys. Rep. **2**, 391.
Wood, C. S., S. C. Bennett, D. Cho, B. P. Masterson, J. L. Roberts, C. E. Tanner, and C. E. Wieman, 1997, Science **275**, 1759.
Yan, Zong-Chao, and G. W. F. Drake, 1995, Phys. Rev. A **52**, R4316.
Zhang, T., and G. W. F. Drake, 1996, Phys. Rev. A **54**, 4882.
Zygelman, B., 1989, in *Relativistic, Quantum Electrodynamic, and Weak Interaction Effects in Atoms*, Santa Barbara, California, 1989, AIP Conf. Proc. No. 189, edited by Walter Johnson, Peter Mohr, and Joseph Sucher (AIP, New York, 1989), p. 408.